© 2019. Published by The Company of Biologists Ltd | Development (2019) 146, dev174292. doi:10.1242/dev.174292

RESEARCH ARTICLE

Strip and *Cka* negatively regulate JNK signalling during *Drosophila* spermatogenesis

John E. La Marca[1,*], Sarah T. Diepstraten[1], Amy L. Hodge[1], Hongyan Wang[2,3,4], Adam H. Hart[1], Helena E. Richardson[1] and W. Gregory Somers[1]

ABSTRACT

One fundamental property of a stem cell niche is the exchange of molecular signals between its component cells. Niche models, such as the *Drosophila melanogaster* testis, have been instrumental in identifying and studying the conserved genetic factors that contribute to niche molecular signalling. Here, we identify *jam packed* (*jam*), an allele of *Striatin interacting protein* (*Strip*), which is a core member of the highly conserved Striatin-interacting phosphatase and kinase (STRIPAK) complex. In the developing *Drosophila* testis, *Strip* cell-autonomously regulates the differentiation and morphology of the somatic lineage, and non-cell-autonomously regulates the proliferation and differentiation of the germline lineage. Mechanistically, *Strip* acts in the somatic lineage with its STRIPAK partner, *Connector of kinase to AP-1* (*Cka*), where they negatively regulate the Jun N-terminal kinase (JNK) signalling pathway. Our study reveals a novel role for *Strip*/*Cka* in JNK pathway regulation during spermatogenesis within the developing *Drosophila* testis.

KEY WORDS: *Drosophila*, Spermatogenesis, Stem cells, Testis, *Strip*, *Cka*, STRIPAK, JNK, TNF, Egr

INTRODUCTION

Adult stem cells are present in most metazoan tissues in specialised microenvironments termed 'niches', where they contribute to the production of differentiated cell populations and are maintained by self-renewal (Li and Xie, 2005). Stem cell identity is maintained by the contribution of molecular signals from the constituent cells of their niche (Li and Xie, 2005). Defective niche signalling can be a contributing factor to tumourigenic stem cell behaviour, leading to unbridled proliferation and self-renewal (Batlle and Clevers, 2017; Cabarcas et al., 2011; Dalerba et al., 2007; Pardal et al., 2003; Reya et al., 2001; White and Lowry, 2014).

One of the earliest identified and now best-studied stem cell niches is the *Drosophila* testis, wherein two stem cell populations – the germline stem cells (GSCs) and somatic cyst stem cells (CySCs) – beget the process of spermatogenesis (Fuller, 1993; Greenspan et al., 2015; Hardy et al., 1979). Physically, each GSC is enclosed by a pair of CySCs, and all adhere to a population of non-mitotic 'hub cells' – these three cell types make up the niche, and the stem cells receive regulatory signals from the hub cells and from each other (Fig. 1A) (Fuller, 1993; Greenspan et al., 2015; Hardy et al., 1979; La Marca and Somers, 2014). Upon dividing asymmetrically, the germline progeny (gonialblasts) exit the niche and undergo four rounds of transit-amplifying (TA) divisions while differentiating, continually enclosed by terminally differentiated CySC progeny: a pair of somatic cyst cells (CyCs) (Fig. 1A) (Fuller, 1993; Greenspan et al., 2015; Hardy et al., 1979). The resultant 16-cell spermatogonial clusters grow and differentiate into spermatocytes, which undergo meiosis and terminal differentiation to produce sperm; however, sperm production does not begin until the white pre-pupal stage, meaning it is not normally observed in third-instar larval (L3) testes (Fig. 1A) (Fuller, 1993; Hardy et al., 1979). The pre-meiotic stages of spermatogenesis are thought to be identical between the developing larval testis/gonad and the adult testis, particularly in terms of the molecular signals regulating stem cell behaviours – these include the Janus kinase-Signal Transducer and Activator of Transcription (Jak-STAT), Transforming Growth Factor β (TGFβ), Hedgehog (Hh), and Epidermal Growth Factor Receptor (EGFR) signalling pathways (Fig. 1A,B) (Matunis et al., 2012; Zoller and Schulz, 2012).

Previous studies using the *Drosophila* testis as a model system have almost exclusively used the adult testis, particularly when screening for genetic regulators of spermatogenesis (Castrillon et al., 1993; Hackstein, 1991; Liu et al., 2016; Matunis et al., 1997; Schulz et al., 2004; Terry et al., 2006). Although such approaches have been undeniably successful, they preclude the identification of genes with additional fundamental roles in organism development and survival. To address this bias, we conducted a forward genetic screen of L3 male gonads from stocks homozygous lethal at the late-larval or pupal stage, which had been generated via EMS mutagenesis on each of the major *Drosophila* chromosomes (Dominado et al., 2016; J.E.L.M., unpublished). Here, we characterise one of the alleles identified in our screen – *jam packed* (*jam*) – which we demonstrate is an allele of *Strip*. *Strip* is a highly conserved core component of the STRIPAK complex (Goudreault et al., 2009; Ribeiro et al., 2010). Although STRIPAK complexes and their components have been implicated in diverse biological roles (Hwang and Pallas, 2014; Kück et al., 2016; Shi et al., 2016), Strip remains relatively poorly understood. We demonstrate that Strip acts within the somatic lineage of the *Drosophila* L3 male gonad, cell-autonomously regulating somatic cell differentiation and morphology, and non-cell-autonomously regulating germline lineage proliferation and differentiation. Furthermore, within the somatic lineage, Strip acts in concert with the core STRIPAK component Cka, and together they bind to a JNK kinase [Hemipterous (Hep)] and act as negative regulators of JNK signalling. *Strip*/*Cka* therefore plays a novel role in regulating the JNK signalling pathway in *Drosophila* spermatogenesis.

[1]Department of Biochemistry and Genetics, La Trobe Institute for Molecular Science, La Trobe University, Bundoora, Victoria, Australia 3086. [2]Neuroscience and Behavioral Disorders Program, Duke-National University of Singapore Graduate Medical School, Singapore 169857. [3]National University of Singapore Graduate School for Integrative Sciences and Engineering, National University of Singapore, Singapore 117456. [4]Department of Physiology, Yong Loo Lin School of Medicine, National University of Singapore, Singapore 117597.

*Author for correspondence (e.lamarca@latrobe.edu.au)

J.E.L.M., 0000-0001-6442-9947

Received 28 November 2018; Accepted 24 May 2019

Development (2019) 146, dev174292. doi:10.1242/dev.174292

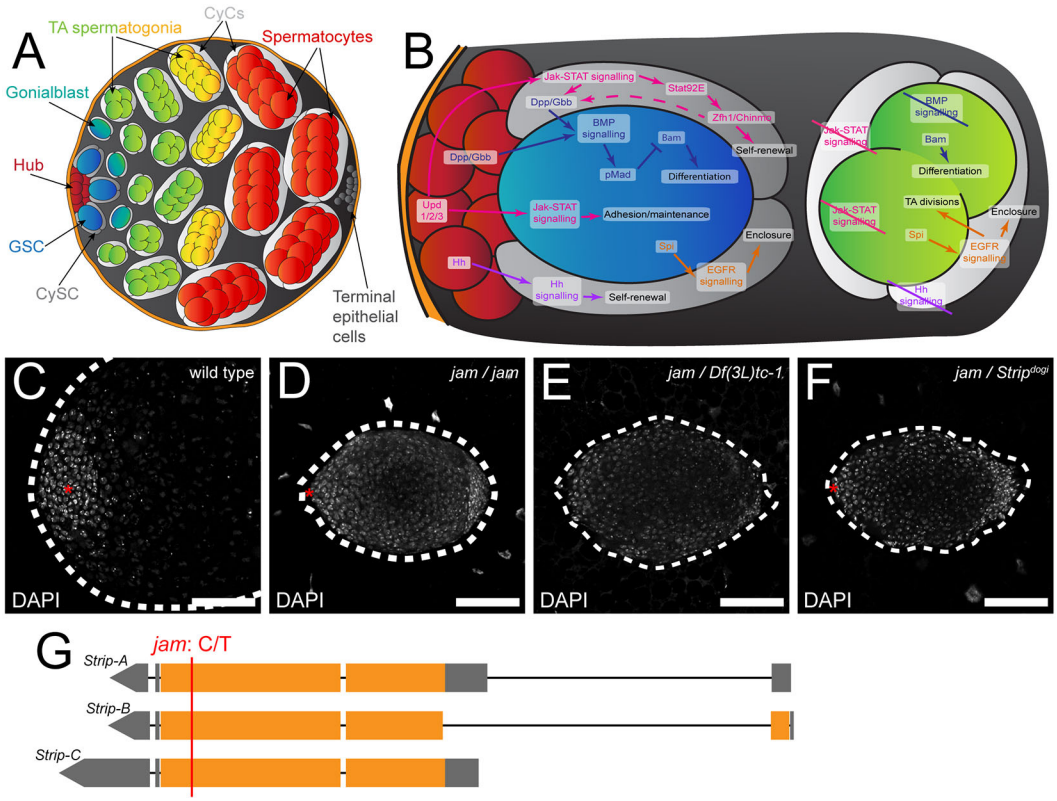

Fig. 1. The L3 male gonad and the identification of *jam packed*. (A) Wild-type *Drosophila* L3 male gonad and spermatogenesis diagram, anterior to the left. Adapted from Dominado et al. (2016). (B) Signalling pathways regulating spermatogenesis within (left) and outside (right) the niche area. (C-F) Gonads from wild-type (C), *jam*/*jam* (D), transheterozygous *jam*/*Df(3L)HR232* (n=6/6) (E) and *jam*/*Strip*^{dogi} (n=16/16) (F) animals stained with DAPI. (G) Sequencing revealed that the *jam* lesion is a C/T substitution in each *Strip* isoform. Where possible, an asterisk marks the hub. Dotted lines outline the gonads. Scale bars: 50 µm.

RESULTS

Identification of the *jam packed* allele

Our forward-genetic screens of late-larval or pupal homozygous lethal mutants searched for those showing defective spermatogenesis in the L3 male gonad (henceforth referred to as 'gonads'). In our screen of 3rd chromosome mutants, we isolated an allele we termed '*jam packed*' (*jam*), after its phenotype (as visualised by DNA staining using DAPI). In wild-type gonads, DAPI-stained DNA appears much brighter in the apical region of the tissue, where the GSCs, gonialblasts, TA spermatogonia, CySCs and CyCs reside (Fig. 1C). By contrast, supernumerary strongly DAPI-positive cells were observed throughout all *jam/jam* gonads (Fig. 1D), which were also significantly smaller than wild-type gonads (Fig. S1A).

In order to identify the gene affected by the *jam* allele, deletion mapping was used to identify a chromosomal region that failed to complement *jam*. A region of lethality was identified between 63D1 and 63D2 on the 3rd chromosome, which contains nine genes, including *Striatin interacting protein* (*Strip*) (Fig. S1B). The *jam/jam* mutant phenotype of supernumerary DAPI-positive cells was strongly recapitulated in gonads from transheterozygous *jam/Df(3L)tc-1* animals (n=6/6) (Fig. 1E) (Sakuma et al., 2014), and transheterozygous *jam/Df(3L)HR232* animals (Fig. S1C). Animals transheterozygous for *jam* and *Strip*^{dogi} (n=16/16) (Fig. 1F), an established null allele of *Strip* (Sakuma et al., 2014), also strongly recapitulated the *jam/jam* phenotype, while those heterozygous for *jam* appeared wild type (Fig. S1D). These data suggested *jam* was an allele of *Strip*.

DNA sequencing of *Strip* in *jam/jam* animals revealed a C/T substitution mutation at base pair 5530 (of the entire gene region), which alters a CAG glutamine codon into a TAG premature stop codon (Fig. 1G). This mutation is present in each predictive isoform of the gene: at base pair 2805 in the transcript of isoforms A, at base pair 2370 in the transcript of isoform B, and at base pair 2542 in the transcript of isoform C. Strip contains two conserved protein domains: a putative transmembrane 'N1221-like domain' and a 'Protein of unknown function DUF3402 domain', in which the *jam* lesion occurs. *Strip* has two mammalian orthologues, *STRIP1* and *STRIP2*, and similar truncation mutations in human *STRIP2* have been identified in a variety of cancer cell lines (Madsen et al., 2015). Our sequencing data predicted that each Strip isoform should be ∼15 kDa smaller in *jam/jam* animals than in the wild type, but western blotting did not detect this change (Fig. S2A), nor did it detect any significant difference in Strip protein levels between the wild type and the mutant (Fig. S2B). The 130 kDa band observed matches the previously reported size for wild-type Strip, which was also observed in embryos homozygous for *Strip*^{dogi} and *Df(3L)tc-1*, which are thought to be null for *Strip* (Sakuma et al., 2014). The observation of this 130 kDa band might be due to aberrant post-translational modifications or the perdurance of maternal Strip in *jam/jam* L3s. Regardless, these data collectively suggest that *jam* is an allele of *Strip*, the disruption of which leads to supernumerary strongly DAPI-positive cells populating the gonads.

Characterisation of *Strip*$^{jam/jam}$ gonad phenotypes

Supernumerary strongly DAPI-positive cells in *Strip*$^{jam/jam}$ gonads suggested the presence of ectopic numbers of early stage cells. Immunofluorescence experiments were performed to identify the lineage of the supernumerary cells and characterise any disruptions to their behaviour/morphology.

Development (2019) 146, dev174292. doi:10.1242/dev.174292

Stem cell character can be rudimentarily denoted by the expression of Escargot (Esg) (Voog et al., 2014). In wild-type gonads (n=14/14), the Esg-GFP reporter marks the hub cells, GSCs, gonialblasts and CySCs (Fig. 2A, arrow). However, in *Strip*$^{jam/jam}$ gonads (n=7/7), Esg-GFP-positive cells were observed throughout the gonad, suggesting the expansion of normally niche-restricted cells (Fig. 2B, arrow). In wild-type gonads (n=17/17), Discs large 1 (Dlg1), a junctional protein, is first detectable at the surfaces of both the germline and somatic cell lineages (Fig. 2C, arrow), before later becoming restricted to the CyCs enclosing the spermatocytes (Fig. 2C, arrowhead) (Papagiannouli and Mechler, 2009). Staining for Dlg1 in *Strip*$^{jam/jam}$ gonads (n=13/13) revealed they contained mainly small individualised cells (Fig. 2D, arrow), with differentiated cysts observed only rarely (Fig. 2D, arrowhead). We next examined two germline lineage markers: Vasa, which marks the entire germline lineage (Hay et al., 1988); and Hu li tai shao (Hts), which marks the spectrosome: a germline-specific organelle (Lighthouse et al., 2008; Lin et al., 1994). In wild-type gonads (n=30/30), staining for Vasa revealed germline cells arranged according to growth and differentiation status, while staining for Hts showed normal spectrosomes (small and round) in the GSCs and gonialblasts, (Fig. 2E,E′, arrows). In TA spermatogonia, spectrosomes were larger and branched (termed fusomes) (Fig. 2E, E′, arrowheads). By contrast, in *Strip*$^{jam/jam}$ gonads (n=27/27), staining for Vasa revealed tissues populated predominantly by small, individualised germline cells containing small, dot-like spectrosomes, rather than branched fusomes (Fig. 2F,F′, arrows). Staining for the hub cell marker Fasciclin 3 (Fas3) did not reveal any obvious differences in hub morphology between the two genotypes (data not shown). Germline differentiation markers were then examined: Bag of marbles (Bam), which marks the TA spermatogonia (Gönczy et al., 1997; Insco et al., 2009; Kawase et al., 2004; Shivdasani and Ingham, 2003); and Matotopetli (Topi), which marks the spermatocytes (Perezgasga et al., 2004). In wild-type gonads (n=31/31), Bam and Topi have a distinct, sequential expression pattern, and clearly mark the differentiating germline (Fig. 2G,G′, arrowheads and arrows). In *Strip*$^{jam/jam}$ gonads (n=21/21), Bam expression was seen in germline cells throughout the gonad, while Topi-expressing cells were rarely observed (Fig. 2H,H′, arrowheads and arrows). Bam expression is repressed by TGFβ signalling, the activity of which is observable by staining for phosphorylated (activated) Mothers against dpp (Mad) (Kawase et al., 2004). Germline pMad expression in wild-type gonads was restricted to the GSCs and gonialblasts (Fig. S3A,A′, arrowheads), while in *Strip*$^{jam/jam}$ gonads it was observed throughout the germline cells (Fig. S3B,B′, arrowheads). Altogether, these data demonstrate *Strip*$^{jam/jam}$ gonads contain supernumerary, largely undifferentiated, germline lineage cells.

We next examined the status of the somatic lineage, first by staining for the CySC/early CyC marker, Zn-finger homeodomain 1 (Zfh1) (Leatherman and DiNardo, 2008), and the germline cell-somatic cell interface marker Armadillo (Arm) (Joti et al., 2011; Sarkar et al., 2007). In wild-type gonads (n=15/15), Zfh1 expression is detectable within the CySCs/early CyCs, as well as in the pigment cells (Fig. 2I, arrowheads), while Arm expression clearly outlined the enclosure of the germline lineage by their somatic cell partners, by marking somatic cell cytoskeletal extensions (Fig. 2I,I′). In contrast, *Strip*$^{jam/jam}$ gonads (n=17/17) showed a loss of germline enclosure, concomitant with a reduction in Arm expression, which was only strongly observed around the tissue border (Fig. 2J,J′, arrows). Additionally, we observed Zfh1-positive cells localised to the surface of the gonads, rather than interspersed between the

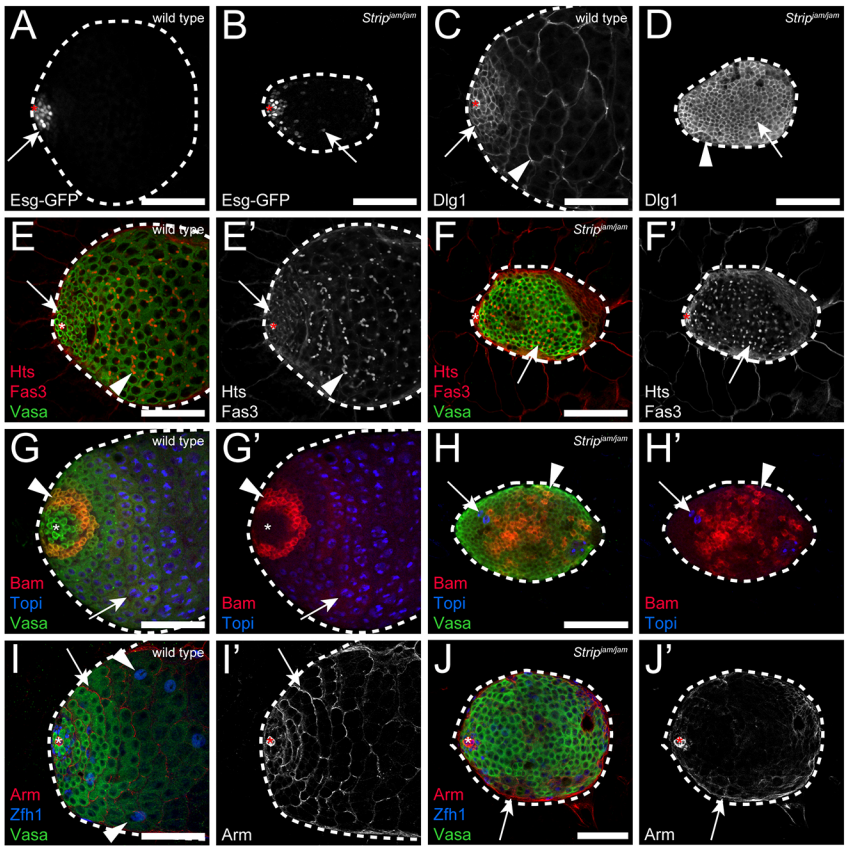

Fig. 2. *Strip* is necessary for proper germline differentiation and somatic cell enclosure. (A,B) Gonads expressing Esg-GFP in wild-type (n=14/14) (A) and *Strip*$^{jam/jam}$ (n=7/7) (B) backgrounds. Arrows indicate Esg-GFP-positive cells. (C,D) Wild-type (n=17/17) (C) and *Strip*$^{jam/jam}$ (n=13/13) (D) gonads stained for Dlg1. Arrows indicate individualised cells; arrowheads indicate cysts. (E-F′) Wild-type (n=30/30) (E,E′) and *Strip*$^{jam/jam}$ (n=27/27) (F,F′) gonads stained for Hts, Fas3 and Vasa. Arrows indicate spectrosomes; arrowheads indicate fusomes. (G-H′) Wild-type (n=31/31) (G,G′) and *Strip*$^{jam/jam}$ (n=21/21) (H,H′) gonads stained for Bam, Topi and Vasa. Arrowheads indicate Bam-positive cells; arrows indicate Topi-positive cells. (I-J′) Wild-type (n=15/15) (I,I′) and *Strip*$^{jam/jam}$ (n=17/17) (J,J′) gonads stained for Arm, Zfh1 and Vasa. Arrows indicate Arm expression; arrowheads indicate Zfh1-positive pigment cells. Where possible, an asterisk marks the hub. Dotted lines outline the gonads. Scale bars: 50 µm.

Development (2019) 146, dev174292. doi:10.1242/dev.174292

germline cells, which suggests a severe disruption to enclosure of the germline lineage by the somatic lineage in *Strip*$^{jam/jam}$ gonads. This lack of Arm staining, and the disruption to somatic cell cytoskeleton organisation it implies, led to our initial investigation of *Strip* as the gene affected by the *jam* mutation: *Strip*, *STRIP1* and *STRIP2* had previously been reported as cytoskeleton regulators *in vitro* (Bai et al., 2011).

To further explore somatic lineage disruptions, we examined expression of the CyC marker, Eyes absent (Eya) (Fabrizio et al., 2003). In wild-type gonads (n=21/21), the somatic lineage transitions from Zfh1 to Eya expression, with a small subpopulation of early CyCs expressing both molecules (Fig. 3A-A″, arrows). Additionally, Eya, unlike Zfh1, does not mark pigment cells (Fig. 3A-A″, arrowheads). Strikingly, in *Strip*$^{jam/jam}$ gonads (n=28/28), the majority of somatic cells were both Zfh1 and Eya positive (Fig. 3B-B″, arrows), and were clearly localised near the surface of the gonads. Additionally, the morphology of the somatic cells was disrupted; their nuclei appeared rounded, rather than having the typical elongated form. Despite these disruptions, some somatic cells were exclusively Zfh1 or Eya positive, and found at the anterior or posterior of the gonad, respectively, suggesting that some cells differentiate normally. These results are supported by staining for Traffic jam (Tj), which, like Zfh1, marks CySCs/early CyCs, but does not mark pigment cells (Li et al., 2003). In wild-type gonads (n=27/27), Tj and Eya sequentially marked the differentiating somatic lineage, with a small region of overlap (Fig. 3C, arrow). Again, contrastingly, in *Strip*$^{jam/jam}$ gonads (n=10/10) the majority of somatic cells were morphologically disrupted and Tj and Eya positive (Fig. 3D, arrows). The Zfh1-/Eya-positive cells at the posterior of each gonad are the somatic terminal epithelial cells (Fig. 3A-D, double arrowheads), which are not thought to contribute to the early stages of spermatogenesis (Fuller, 1993). Finally, we observed strong expression of pMad in the somatic cells pushed to the surface of *Strip*$^{jam/jam}$ gonads (Fig. S3C,C′, arrows), where it is normally restricted to CyCs in the wild type (Fig. S3A,A′, arrows). These data demonstrate that the differentiation and morphology of somatic lineage cells in *Strip*$^{jam/jam}$ gonads is disrupted.

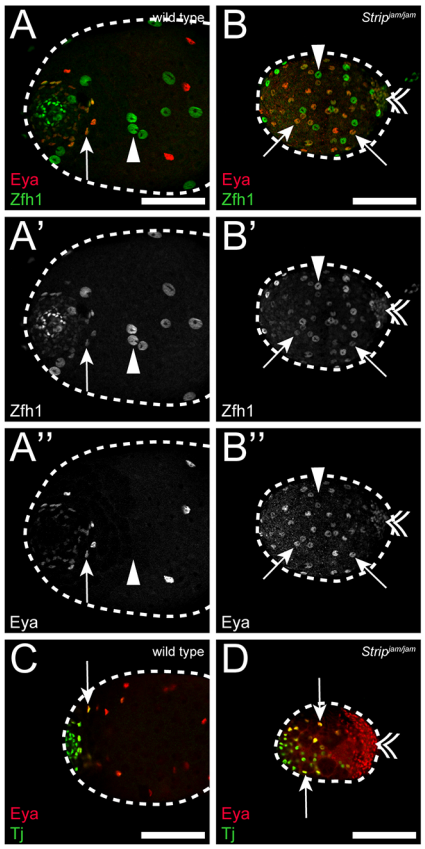

Fig. 3. Somatic cell differentiation and morphology is disrupted in *Strip*$^{jam/jam}$ gonads. (A-B″) Wild-type (n=21/21) (A-A″) and *Strip*$^{jam/jam}$ (n=28/28) (B-B″) gonads stained for Eya and Zfh1. Arrows indicate Zfh1- and Eya-positive somatic cells; arrowheads indicate Zfh1-positive pigment cells; double arrowheads indicate terminal epithelial cells. (C,D) Wild-type (n=27/27) (C) and *Strip*$^{jam/jam}$ (n=10/10) (D) gonads stained for Eya and Tj. Arrows indicate Tj- and Eya-positive somatic cells. Dotted lines outline the gonads. Scale bars: 50 µm.

Altogether, these results suggest *Strip*$^{jam/jam}$ L3 gonads are primarily populated by supernumerary, largely undifferentiated, germline lineage cells. Additionally, somatic lineage differentiation and morphology is disrupted, and germline enclosure by the somatic lineage is disrupted.

Proliferation and cell death are severely disrupted in *Strip*$^{jam/jam}$ gonads

The presence of supernumerary germline cells in *Strip*$^{jam/jam}$ gonads suggested that some cells might be overproliferating. To investigate, we pulse-labelled dissected gonads with BrdU to detect cells undergoing DNA replication. In wild-type gonads (n=22/22), BrdU incorporation was consistently observed only in those cells in the apical region of the gonad (Fig. 4A), whereas in *Strip*$^{jam/jam}$ gonads (n=31/32), we observed BrdU-positive cells throughout the tissue (Fig. 4B). Staining for the M-phase marker phosphorylated Histone H3 (pHis3), gave similar results: in wild-type gonads (n=39/39), individualised pHis3-positive cells (indicative of dividing GSCs or gonialblasts) (Fig. 4C, arrow), as opposed to clusters of pHis3-positive cells (indicative of dividing spermatogonia) (Fig. 4C, arrowhead), were only ever observed within the apical region. By contrast, in *Strip*$^{jam/jam}$ gonads (n=50/50), individualised pHis3-positive cells were observed throughout the tissue. These data support the hypothesis of overproliferation occurring in *Strip*$^{jam/jam}$ gonads.

To precisely identify the overproliferating cells, we undertook co-staining for pHis3, Zfh1 and Vasa, which, respectively, mark the proliferating cells, the somatic lineage and the germline lineage. By quantifying each pHis3-positive cell and its lineage, statistical analyses revealed that the difference in the average number (±s.e.m.) of pHis3-/Zfh1-positive cells between wild-type (0.26±0.080) and *Strip*$^{jam/jam}$ (0.28±0.076) gonads is negligible (Student's t-test, P>0.05) (Fig. 4E). Antithetically, the average number of cells that are pHis3 and Vasa positive in wild-type (0.97±0.17) and *Strip*$^{jam/jam}$ (15.12±1.12) gonads is significantly different (Student's t-test, P<0.001) (Fig. 4E), indicating the germline lineage is overproliferating in *Strip*$^{jam/jam}$ gonads. We next sought to dissect the composition of the germline lineage. Quantification of the different stages of proliferating germline cells revealed that, in wild-type gonads, the percentages of cells proliferating individually (28.95%) or as clusters of two cells (21.05%), four cells (23.68%) and eight cells (23.68%) are roughly equal, while a lower percentage of cells are proliferating in 16-cell clusters (2.64%) (Fig. 4F). By contrast, in *Strip*$^{jam/jam}$ gonads, the percentage of germline cells proliferating individually (84.43%) is conspicuously larger than the percentage of those proliferating as two (12.53%), four (2.38%), eight (0.40%) and 16 (0.26%) cell clusters (Fig. 4F). Taken together, these data demonstrate that the majority of germline cells in *Strip*$^{jam/jam}$ gonads are individualised cells undergoing ectopic proliferation, while also failing to undergo TA divisions or differentiate.

Development (2019) 146, dev174292. doi:10.1242/dev.174292

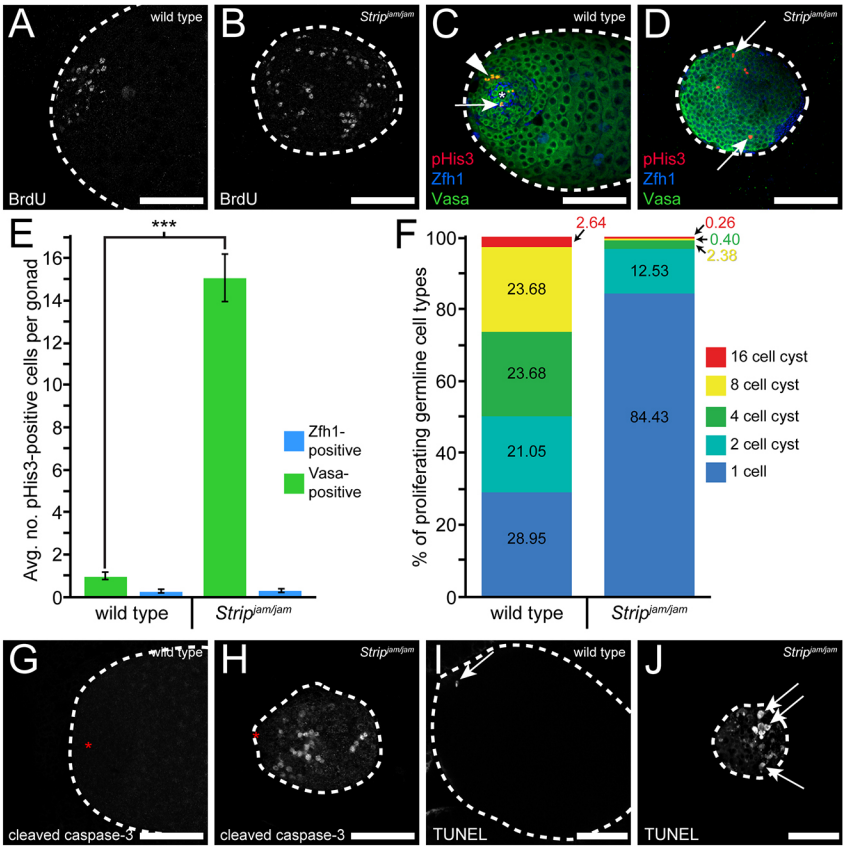

Fig. 4. *Strip*$^{jam/jam}$ gonads possess ectopic levels of germline proliferation and apoptosis. (A,B) Wild-type (n=22/22) (A) and *Strip*$^{jam/jam}$ (n=31/32) (B) gonads stained for incorporated BrdU. (C,D) Wild-type (n=39/39) (C) and *Strip*$^{jam/jam}$ (n=50/50) (D) gonads stained for pHis3, Zfh1 and Vasa. Arrows indicate individualised pHis3-positive germline cells; arrowhead indicates a pHis3-positive germline cluster. (E) Quantification of pHis3-positive cells in wild-type and *Strip*$^{jam/jam}$ gonads. Significantly more proliferating germline cells were observed in *Strip*$^{jam/jam}$ gonads (***P<0.001, Student's t-test). Data are mean±s.e.m. (F) Quantification of the proliferating germline stages in wild-type and *Strip*$^{jam/jam}$ gonads. (G,H) Wild-type (n=15/15) (G) and *Strip*$^{jam/jam}$ (n=14/14) (H) gonads stained for cleaved Caspase-3/Dronc. (I,J) Wild-type (n=5/5) (I) and *Strip*$^{jam/jam}$ (n=10/10) (J) gonads after TUNEL. Arrows indicate apoptotic cells. Where possible, an asterisk marks the hub. Dotted lines outline the gonads. Scale bars: 50 µm.

Ectopic proliferation could be expected to lead to larger than normal gonads due to increased cell numbers. As *Strip*$^{jam/jam}$ gonads were, without exception, smaller than wild-type gonads, we hypothesised that cell death was elevated in *Strip*$^{jam/jam}$ gonads. Accordingly, we marked dying cells using an antibody against human cleaved caspase 3, which indicates the activity of the apoptosis protein Death regulator Nedd2-like caspase (Dronc) in *Drosophila* (Fan and Bergmann, 2010). In wild-type gonads (n=15/15), we saw no Dronc/cleaved Caspase 3 expression (Fig. 4G), which strongly contrasts with the large number of Dronc/cleaved Caspase 3-positive cells observed in *Strip*$^{jam/jam}$ gonads (n=14/14) (Fig. 4H). TUNEL assays gave similar data, demonstrating negligible apoptosis levels in wild-type gonads (n=5/5) (Fig. 4I, arrow), but large numbers of apoptotic cells in *Strip*$^{jam/jam}$ gonads (n=10/10) (Fig. 4J, arrows). These data suggest that the reduced size of *Strip*$^{jam/jam}$ gonads might be due to increased cell death.

Strip acts in the somatic lineage to regulate spermatogenesis

In order to identify the lineage(s) in which *Strip* is necessary, as well as confirm the identity of *jam* as a *Strip* allele, we utilised the *GAL4/UAS* system to induce cell-specific transgene expression. Using the *C587-GAL4* driver, which induces expression in the early somatic cells (Demarco et al., 2014), and co-expressing *Dicer-2* (*Dcr-2*), a known positive regulator of the RNA interference (RNAi) process (Kim et al., 2006), we found that the knockdown of *Strip* via RNAi lines v16211 (n=14/21 at 25°C, n=9/10 at 29°C) (Fig. 5A,A′) and v16212 (n=12/14 at 25°C, n=12/12 at 29°C) (Fig. 5B,B′) strongly recapitulated the *Strip*$^{jam/jam}$ gonad phenotypes. Knockdown of *Strip* in either the hub or germline lineages (Fig. S4A-B′), using the drivers *unpaired 1-GAL4* (*upd1-GAL4*) and *nanos-GAL4; UAS-GAL4* (hereafter *nos-GAL4*), respectively, did not yield any aberrant phenotypes. The somatic lineage specificity of *Strip* was further confirmed by replicating the *Strip*$^{jam/jam}$-like phenotype using *traffic jam-GAL4* (*tj-GAL4*), another early somatic cell-specific driver, and RNAi line v16212 against *Strip* (Fig. S4E,E′).

We generated transgenic constructs containing wild-type *Strip*, under *UAS* control, tagged with a *YFP* variant: *Venus* (Nagai et al., 2002). Two independent insertion lines of this transgene were examined: *UAS-Strip-YFP#1* and *UAS-Strip-YFP#2*. Somatic cell expression of *UAS-Strip-YFP#1* (n=22/22) in a wild-type background had no obvious effect on spermatogenesis (Fig. 5C,C′,E,E′). Significantly, somatic cell expression of *UAS-Strip-YFP#1* in a *Strip*$^{jam/jam}$ background (n=37/37) almost completely rescued the mutant phenotype (Fig. 5D,D′,F,F′), with germline differentiation and somatic cell morphology/differentiation appearing restored. Lethality was not rescued, likely owing to limited expression of the *C587-GAL4* driver. Similar results were obtained after somatic cell expression of *UAS-Strip-YFP#2* in both wild-type and *Strip*$^{jam/jam}$ backgrounds (Fig. S5A-D′). Additionally, *Strip-YFP* expression in the somatic lineage rescued gonad size, with line #1 the more effective (Fig. S5E). Germline divisions were not rescued completely after *Strip-YFP* expression – TA spermatogonia and spermatocytes appeared to contain two cells at most, rather than 16 (Fig. 5D,D′, arrows). This may be due to Strip-YFP lacking some functionality, insufficient expression levels for *Strip-YFP*, dominant-negative behaviour of *Strip*^{jam} or some minor germline lineage role for *Strip*. Note, however, that expression of *Strip-YFP#1* in the germline using *nos-GAL4* had no discernible effect on the wild-type or *Strip*$^{jam/jam}$ phenotypes (Fig. S5F-G′). Collectively, the identification of the molecular lesion in *Strip*^{jam} by DNA sequencing, the phenocopying of the *Strip*$^{jam/jam}$ gonad phenotypes in

Development (2019) 146, dev174292. doi:10.1242/dev.174292

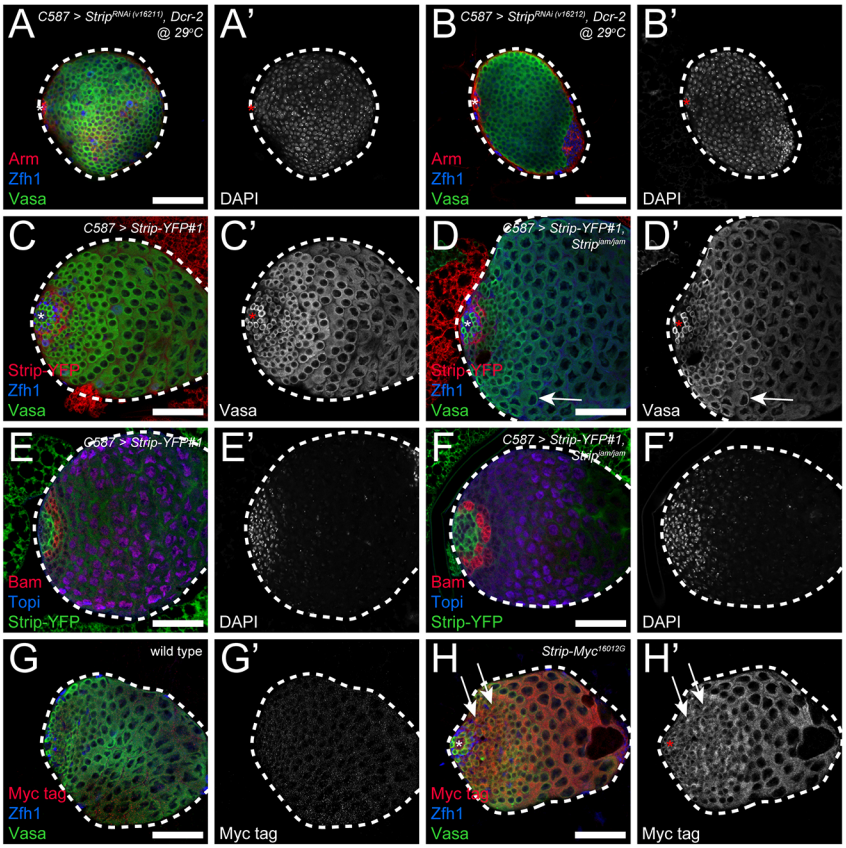

Fig. 5. *jam* is an allele of *Strip*, which is necessary in the somatic lineage. (A-B′) Gonads with somatic lineage co-expression of *Dcr-2* and RNAi against *Strip* – v16211 (*n*=14/21 at 25°C, *n*=9/10 at 29°C) (A,A′) and v16212 (*n*=12/14 at 25°C, *n*=12/12 at 29°C) (B,B′) – stained for Arm, Zfh1 and Vasa, and with DAPI. (C-F′) Gonads with somatic lineage expression of *Strip-YFP#1* in both wild-type (*n*=22/22) (C,C′,E,E′) and *Strip*$^{jam/jam}$ (*n*=37/37) (D,D′,F,F′) backgrounds, stained for Zfh1 and Vasa, or for Bam and Topi with DAPI. Arrows indicate an individualised, yet differentiated, germline cell. (G-H′) Wild-type (*n*=13/13) (G,G′) and *Strip-Myc*^{16012G} (*n*=22/22) (H,H′) gonads stained for the Myc epitope tag, Zfh1 and Vasa. Arrows indicate patches of strong Strip-Myc expression. Where possible, an asterisk marks the hub. Dotted lines outline the gonads. Scale bars: 50 µm.

transheterozygous and *Strip* RNAi knockdown larvae and the partial rescue of *Strip*$^{jam/jam}$ mutant phenotypes by expression of *Strip-YFP* all contribute to the confirmation of *jam* as a *Strip* allele. Additionally, RNAi and *Strip-YFP* transgene data indicate that *Strip* acts in the somatic lineage to autonomously regulate somatic cell differentiation and morphology, and non-cell-autonomously to regulate germline differentiation.

As we were unable to detect Strip *in vivo* with any available antibodies, we employed clustered regularly interspaced short palindromic repeats/CRISPR associated protein 9 (CRISPR/Cas9) gene-editing technology to tag endogenous *Strip* (Fig. S6A-E). We generated multiple homozygous viable stocks containing a *3×Myc tag* sequence at the 3′ end of the *Strip* CDS, which is shared across each isoform. Immunofluorescence against the Myc tag epitope showed only background staining in wild-type gonads (*n*=13/13) (Fig. 5G,G′), but gonads from the CRISPR/Cas9-generated *Strip-Myc*^{16012G} stock (*n*=22/22) revealed cytoplasmic Strip-Myc expression in each gonad lineage (Fig. 5H,H′). Patches of stronger expression were noticeable in the spermatogonia, localised next to their nuclei (Fig. 5H,H′, arrows), possibly indicative of localisation to the endoplasmic reticulum, where orthologues of Strip localise in both yeasts and *Caenorhabditis elegans* (Frost et al., 2012; Maheshwari et al., 2016). Strip-Myc was also observed in the cytoplasm of the CySCs and CyCs, but, owing to their extremely narrow morphologies, more-specific localisation was not able to be discerned. Notably, these findings were replicated when using *Strip-Myc*$^{2\text{-}38\text{-}4\text{-}1}$ lines concurrently generated by Takahiro Chihara (Fig. S6F-G″) (Sakuma et al., 2016).

Strip and *Cka* interact physically while regulating spermatogenesis

Strip is a core member of the highly conserved, but poorly understood, STRIPAK complex – in *Drosophila*, the STRIPAK complex has an array of dynamic subunits, including phosphatase components [Protein phosphatase 2A at 29B (Pp2A-29B) and Microtubule star (Mts)], kinase components [Germinal centre kinase III (GckIII), Misshapen (Msn)], structural subunits [Cka, Strip, MOB kinase activator 4 (Mob4)] and other subunits with less-well defined roles [e.g. Fibroblast growth factor receptor 1 oncogene partner 2 (Fgop2), Cerebral cavernous malformation 3 (Ccm3), Sarcolemma associated protein (Slmap)] (Fig. 6A) (Ashton-Beaucage et al., 2014; Guruharsha et al., 2011; Hwang and Pallas, 2014; Ribeiro et al., 2010). At the core of the complex is Cka, an orthologue of the human striatin proteins (STR, STR3, STR4). Therefore, we questioned whether knockdown of *Cka* via RNAi might replicate the phenotypes seen upon *Strip* knockdown/mutation. Knockdown of *Cka* in the somatic lineage via RNAi lines v35234 (*n*=10/10) (Fig. 6B,B′) and v106971 (*n*=9/22 at 25°C, *n*=5/7 at 29°C) (Fig. 6C,C′), while co-expressing *Dcr-2*, successfully recapitulated the *Strip* knockdown/mutation gonad phenotypes. Knockdown of *Cka* in the hub or germline lineages had, like *Strip* knockdown, no effect on the gonad phenotype (Fig. S4C-D′). However, somatic cell-specific knockdown of the STRIPAK complex members *Fgop2*, *GckIII*, *Mob4*, *msn* and *Slmap*, via RNAi, had no effect on spermatogenesis (Fig. S7A-F′), even with *Dcr-2* co-expression. Owing to this negative result, we confirmed the efficacy of each RNAi via quantitative reverse transcription PCR (RT-qPCR) (Fig. S7G). RNAi lines against *Ccm3* (v106841) and *mts* (v35171) were also tested *in vivo* and via RT-qPCR, but were found to be non-functional (data not shown). An exception was the case of somatic cell knockdown of *Pp2A-29B*, which induced a loss of early germline cells (Fig. S8A-B′), a phenotype distinct from that observed for *Strip* and *Cka* knockdown.

We next explored whether Strip and Cka interacted physically in L3 tissues via co-immunoprecipitation experiments. In wild-type L3 tissue extracts, we demonstrated that Strip and Cka both

Development (2019) 146, dev174292. doi:10.1242/dev.174292

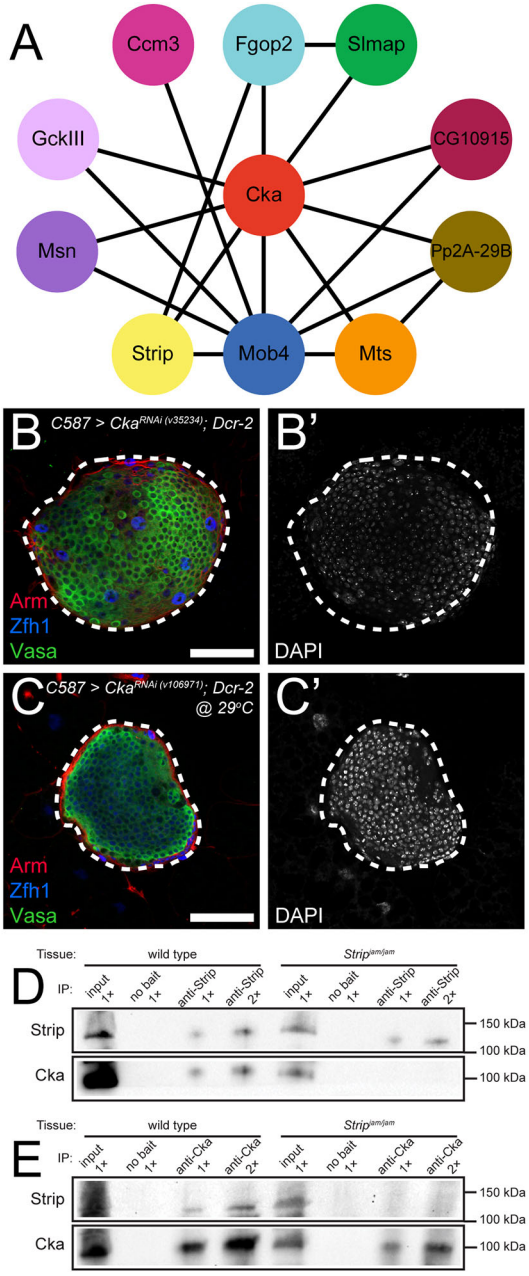

Fig. 6. Cka has a role in spermatogenesis and physically interacts with Strip. (A) Diagram representing known physical interactions between STRIPAK complex members. (B-C′) Gonads with somatic lineage co-expression of *Dcr-2* and RNAi against *Cka* – v35234 (*n*=10/10) (B,B′) and v106971 (*n*=9/22 at 25°C, *n*=5/7 at 29°C) (C,C′) – stained for Arm, Zfh1 and Vasa, and with DAPI. (D,E) In wild-type tissue extracts, but not in *Strip*$^{jam/jam}$ tissue extracts, Cka immunoprecipitated when baited with anti-Strip (performed four times) (D), and Strip immunoprecipitated when baited with anti-Cka (performed twice) (E). Dotted lines outline the gonads. Scale bars: 50 µm.

immunoprecipitated when baited with antibodies against the other (Fig. 6D,E, lanes 3,4). In *Strip*$^{jam/jam}$ L3 tissue extracts, although Strip and Cka were detected following immunoprecipitation with their respective antibodies, the Strip-Cka physical interaction was not observed (Fig. 6D,E, lanes 7,8). These data suggest that Strip and Cka physically interact in the wild-type, but the *Strip*^{jam} mutation precludes this interaction. Potentially, the *Strip*$^{jam/jam}$ mutant gonad phenotypes derive from this defective interaction. These data suggest that physical interactions between Strip and Cka contribute to proper somatic cell differentiation, morphology and behaviour.

Strip, Cka, and other STRIPAK components have been shown to act as positive regulators of EGFR signalling in the *Drosophila* wing and eye, and *in vitro* (Ashton-Beaucage et al., 2014; Friedman and Perrimon, 2006; Horn et al., 2011; Wassarman et al., 1996). Additionally, EGFR signalling is an established regulator of somatic cell enclosure and morphology, and of germline differentiation during spermatogenesis (Fig. S9A) – indeed, disrupting *Strip*, *Cka*, or EGFR signalling pathway components yielded strikingly similar gonad phenotypes (Chen et al., 2013; Hudson et al., 2013; Kiger et al., 2000; Sarkar et al., 2007; Schulz et al., 2002; Tran et al., 2000). Therefore, we wanted to explore whether *Strip* interacted genetically with the EGFR signalling pathway. We first examined EGFR pathway activity, as measured by phosphorylated Rl (also known as ERK/MAPK) abundance, which appeared similar between the wild-type and *Strip*$^{jam/jam}$ gonads (Fig. S9B-C′). We next examined whether EGFR signalling suppression phenotypes could be worsened by the presence of *Strip*^{jam} (Fig. S9D-E′), and also whether *Strip*$^{jam/jam}$ gonad phenotypes could be rescued by EGFR pathway activation (Fig. S9F-I′), but observed no genetic interactions. These data suggested that, rather than interacting with EGFR signalling, a pathway with an established role in spermatogenesis that *Strip* is known to regulate, *Strip* has some alternate mode of action.

Strip and *Cka* interact genetically with JNK signalling to regulate spermatogenesis

Cka was originally identified as a positive regulator of c-Jun N-terminal kinase (JNK) signalling, which mediates the physical interactions between Hep, a JNKK, Basket (Bsk), the sole *Drosophila* JNK, and the AP-1 transcription factor complex, which consists of Jun-related antigen (Jra) and Kayak (Kay) (Fig. 7A) (Chen et al., 2002). The JNK signalling core of Hep and Bsk can be activated by a number of pathways, one of which is the immune deficiency (IMD) signalling pathway (Fig. 7A) (Hoffmann, 2003; Kaneko and Silverman, 2005). Interestingly, it has been demonstrated that Strip, Cka and other STRIPAK components act as negative regulators of JNK signalling when the pathway is activated by IMD signalling after peptidoglycan administration (Ashton-Beaucage et al., 2014; Bond and Foley, 2009). We hypothesised, therefore, that Strip and Cka might be acting as negative regulators of JNK signalling during spermatogenesis.

We first examined staining for phosphorylated JNK (pJNK), which marks JNK signalling activation. Although low in wild-type gonads (*n*=8/8) (Fig. 7B), pJNK levels were clearly elevated in *Strip*$^{jam/jam}$ gonads (*n*=11/11), particularly in the somatic cells at the gonad surface (Fig. 7C, arrows). Consistent with this were the levels of Matrix metalloproteinase 1 (Mmp1), an established target of JNK signalling (Uhlirova and Bohmann, 2006), which was restricted to the somatic cells and only weakly expressed in somatic cells in wild-type gonads (Fig. S10A, arrow), but strongly expressed in *Strip*$^{jam/jam}$ gonads (Fig. S10B, arrow). These data indicate that JNK signalling is elevated specifically in the somatic lineage in *Strip*$^{jam/jam}$ animals.

As Cka can act as a scaffold for the physical interactions of Hep, Bsk and the AP-1 complex (Chen et al., 2002), we examined whether Cka and Strip interact physically with Hep in wild-type and *Strip*$^{jam/jam}$ L3 tissues via co-immunoprecipitation. We observed that in L3 tissue extracts from both genotypes, Hep immunoprecipitated when baited with antibodies against either Cka or Strip (Fig. S10C,D, lanes 3,4,7,8). This suggests that Hep

Development (2019) 146, dev174292. doi:10.1242/dev.174292

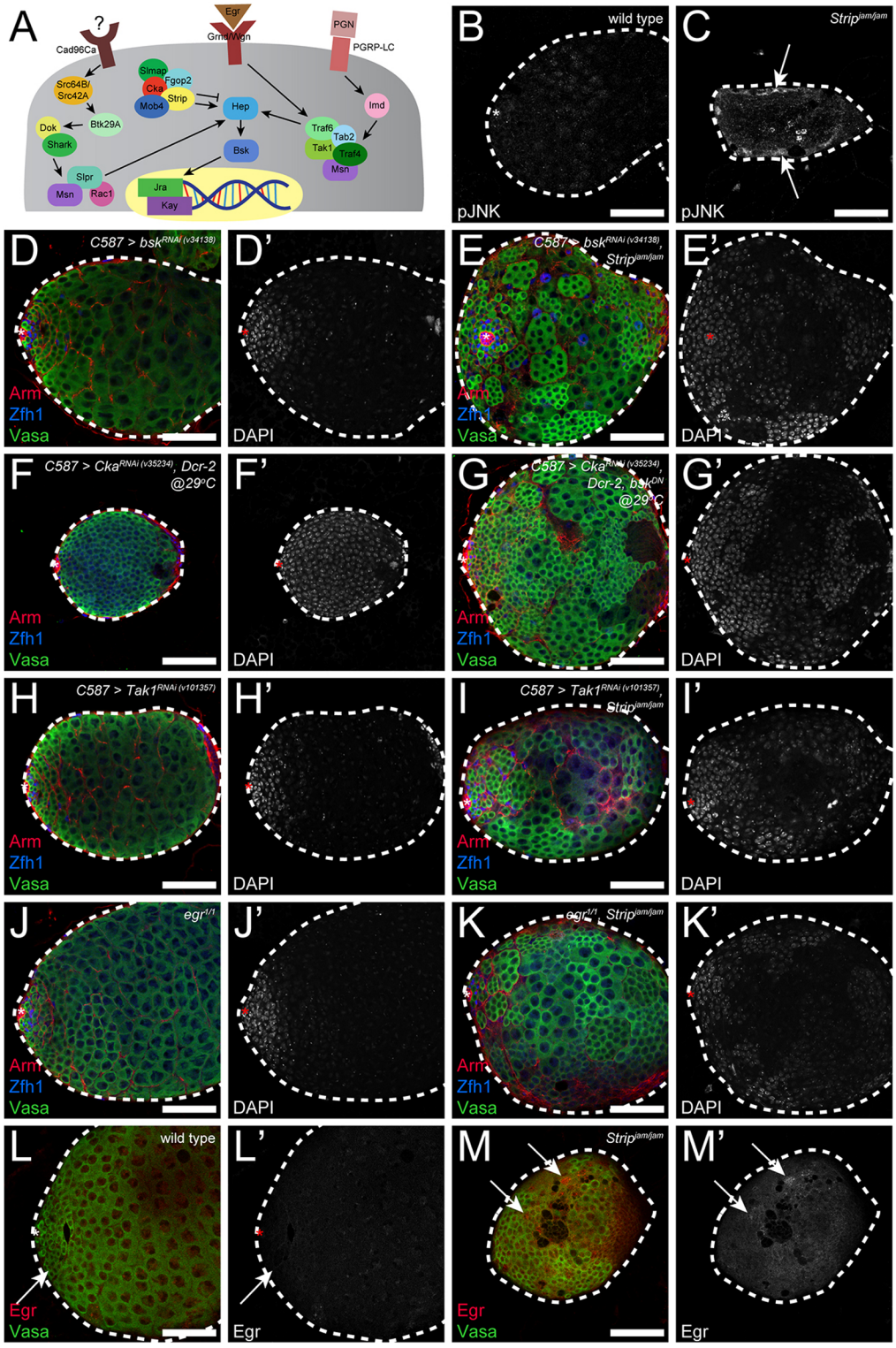

Fig. 7. *Strip* genetically interacts with the TNF-JNK signalling pathway in the gonad. (A) Diagram of *Drosophila* JNK signalling pathways. Depending on activation context, STRIPAK complex members have been shown to positively or negatively regulate JNK signalling. (B,C) Wild-type (n=8/8) (B) and $Strip^{jam/jam}$ (n=11/11) (C) gonads stained for pJNK. Arrows indicate pJNK expression. (D-I′) Gonads from animals with somatic lineage expression of various transgenes, stained for Arm, Zfh1 and Vasa, and with DAPI. (D-E′) Expressing RNAi against *bsk* in both wild-type (n=9/9) (D,D′) and $Strip^{jam/jam}$ (n=15/15) (E,E′) backgrounds. (F-G′) Co-expressing *Dcr-2* and RNAi against *Cka* (v35234) in wild-type (v35234, n=6/7; v106971, n=10/15) (F,F′) and bsk^{DN}-expressing (v35234, n=10/13; v106971, n=13/16) (G,G′) backgrounds. (H-I′) Expressing RNAi against *Tak1* in both wild-type (n=14/14) (H,H′) and $Strip^{jam/jam}$ (n=22/22) (I,I′) backgrounds. (J-K′) Gonads from animals homozygous for egr^{1} in wild-type (n=12/12) (J,J′) and $Strip^{jam/jam}$ (n=15/15) (K,K′) backgrounds, stained for Arm, Zfh1 and Vasa, and with DAPI. (L-M′) Wild-type (n=59/59) (L,L′) and $Strip^{jam/jam}$ (n=58/58) (M,M′) gonads stained for Egr and Vasa. Arrows indicate Egr expression; low in the wild-type gonad somatic lineage, higher in the $Strip^{jam/jam}$ gonad somatic lineage. Where possible, an asterisk marks the hub. Dotted lines outline the gonads. Scale bars: 50 µm.

physically interacts with Cka and Strip in both wild-type and $Strip^{jam/jam}$ tissues, despite our observation that Strip^{jam} precludes Cka and Strip themselves from physically interacting (Fig. 6D,E).

We next examined whether reducing JNK signalling via knockdown of Bsk might partially rescue the $Strip^{jam/jam}$ gonad phenotype. In a wild-type background (n=9/9), expression of RNAi against *bsk* in the somatic lineage did not modify the L3 gonad phenotype (Fig. 7D,D′). By contrast, somatic cell expression of RNAi against *bsk* in a $Strip^{jam/jam}$ background (n=15/15) led to a partial rescue of the mutant phenotype, with proper germline differentiation and somatic cell enclosure clearly visible (Fig. 7E,E′). These results were replicated upon somatic lineage expression of a dominant-negative bsk^{DN} transgene: in a wild-type background bsk^{DN} had no discernible effect (Fig. S10E,E′), whereas in a $Strip^{jam/jam}$ background bsk^{DN} partially rescued the phenotype (Fig. S10F,F′). Furthermore, somatic lineage expression of bsk^{DN} rescued the altered

Development (2019) 146, dev174292. doi:10.1242/dev.174292

expression patterns of Bam and Topi observed in the mutant gonads (Fig. S10G,H), and both methods of *bsk* disruption significantly increased the size of *Strip*$^{jam/jam}$ gonads (Fig. S10I). Furthermore, we examined whether knockdown of *bsk* might rescue phenotypes induced by *Cka* knockdown. As before, in a wild-type background, somatic cell co-expression of *Dcr-2* and RNAi against *Cka* (v35234, *n*=6/7 and v106971, *n*=10/15) phenocopied the *Strip*$^{jam/jam}$ gonad phenotype (Fig. 7F,F′). Knockdown of *Cka* together with expression of the *bsk*^{DN} transgene (v35234, *n*=10/13 and v106971, *n*=13/16) led to a striking partial rescue of the germline differentiation and somatic cell enclosure defects of *Cka* knockdown (Fig. 7G,G′). Collectively, these data indicate that *Strip* and *Cka* mutant/knockdown phenotypes are rescued by reducing JNK signalling activity, suggesting that *Strip* and *Cka* negatively regulate JNK signalling in the *Drosophila* gonad.

Previously, *Strip* and *Cka* have been shown to negatively regulate JNK signalling initiated via IMD signalling (Ashton-Beaucage et al., 2014; Bond and Foley, 2009). IMD signalling proceeds via the receptor PGRP-LC, which activates Immune deficiency (Imd) and, in turn, activates the kinase complex containing Misshapen (Msn, a JNKKKK), TGFβ activated kinase 1 (Tak1, a JNKKK) and their binding partners: TAK1-associated binding protein 2 (Tab2), TNF-receptor-associated factor 4 (Traf4) and TNF-receptor-associated factor 6 (Traf6) (Fig. 7A). Somatic cell expression of an RNAi line against *imd* was unable to rescue the *Strip*$^{jam/jam}$ gonad phenotype (Fig. S11A-B′), with the RNAi efficacy confirmed via RT-qPCR (Fig. S11C), suggesting Imd activation is not the source of the JNK signalling. However, as alternative activators of Tak1 exist, we examined it directly. In a wild-type background (*n*=14/14), expression of RNAi against *Tak1* in the somatic lineage did not alter the gonad phenotype (Fig. 7H,H′), but in a *Strip*$^{jam/jam}$ background (*n*=22/22), we again observed a partial rescue of the mutant phenotypes (Fig. 7I,I′). Similarly, somatic cell knockdown of *Traf6* led to a partial rescue (Fig. S10J-K′).

The Tumour Necrosis Factor (TNF) signalling pathway uses Tak1 to activate JNK signalling, and is initiated by the ligand, Eiger (Egr), binding to either of its receptors: Grindelwald (Grnd) and Wengen (Wgn) (Fig. 7A) (Andersen et al., 2015; Igaki et al., 2002; Igaki and Miura, 2014; Vidal, 2010). To explore a role for TNF signalling, two mutant alleles of *egr* were used: *egr*^{1} and *egr*^{3}. In an otherwise wild-type background, *egr*$^{1/1}$ (*n*=12/12) (Fig. 7J,J′) and *egr*$^{3/3}$ (Fig. S10L,L′) gonads appeared normal, whereas in a *Strip*$^{jam/jam}$ background the mutant gonad phenotypes were partially rescued by the presence of *egr*$^{1/1}$ (*n*=15/15) (Fig. 7K,K′) and *egr*$^{3/3}$ (Fig. S10M,M′). Therefore, we hypothesised that Egr expression might be elevated in *Strip*$^{jam/jam}$ gonads relative to the wild type. In wild-type gonads (*n*=59/59), only low levels of CyC-specific Egr expression was observed (Fig. 7L,L′, arrows). By contrast, in *Strip*$^{jam/jam}$ gonads (*n*=58/58), elevated Egr expression was observed in the somatic cells at the gonad surface (Fig. 7M,M′, arrows), and occasionally in the cytoplasm of the supernumerary germline cells (Fig. S12A,A′, arrows). Egr can be secreted by haemocyte cells identifiable by Nimrod C1 (NimC1) expression (Fogarty et al., 2016), although no NimC1-positive cells were present in either wild-type or *Strip*$^{jam/jam}$ gonads (data not shown), suggesting Egr is secreted from another lineage, or acts autocrinically within the somatic lineage. Interestingly, lineage-specific expression of *egr* in the somatic (Fig. S12B,B′), germline (Fig. S12C,C′) or hub (Fig. S12D,D′) cells did not alter the gonad phenotypes. This suggests overexpression of Egr might not be sufficient to recapitulate the *Strip*$^{jam/jam}$ mutant phenotypes, or that in a wild-type background, functional *Strip* might suppress any elevated Egr activity. Finally, we examined Egr expression in gonads expressing *bsk*^{DN} in somatic cells: in an otherwise wild-type background, Egr expression appeared normal (Fig. S12E,E′), whereas in a *Strip*$^{jam/jam}$ background, where the mutant phenotype was partially rescued, the ectopic Egr expression seen in non-rescued mutant gonads was absent (Fig. S12F,F′). Collectively, these data indicate that TNF-JNK signalling driven by Egr is upregulated in *Strip*$^{jam/jam}$ gonads, and that blocking JNK signalling both rescues the mutant phenotype and reduces expression of Egr.

DISCUSSION

In this study, we have identified *jam*, a novel allele of the poorly understood gene *Strip*, and have characterised the role of *Strip* in the *Drosophila* L3 male gonad. We found that *Strip* acts in the somatic lineage of the gonad, where it cell-autonomously regulates the differentiation and morphology of the somatic cells, and their ability to encapsulate cells of the germline lineage. Non-cell-autonomously, *Strip* regulates the proliferation and differentiation of the germline lineage. Mechanistically, Strip acts with Cka to physically interact with Hep (JNKK) and negatively regulate TNF-JNK signalling in the somatic cells during spermatogenesis.

Previous studies, largely performed *in vitro*, have demonstrated JNK signalling is regulated both positively and negatively by STRIPAK complex members (Ashton-Beaucage et al., 2014; Bond and Foley, 2009; Chen et al., 2002). However, Strip and its orthologues also act in a diversity of roles distinct from JNK signalling, both in isolation and with members of the STRIPAK complex. For example, in yeasts, the FAR complex (STRIPAK complex equivalent) has been implicated in cell-cycle arrest in response to pheromones (Kemp and Sprague, 2003), while the Strip orthologue FAR11 regulates Caspase-10-induced cell death (Lisa-Santamaría et al., 2012) and inhibits TORC2 signalling (Pracheil and Liu, 2013; Pracheil et al., 2012). In mammals, STRIP1 and STRIP2 have roles in cytoskeletal organisation (Bai et al., 2011; Rohn et al., 2011), Hippo signalling regulation and cell migration (Madsen et al., 2015), and embryogenesis (Bazzi et al., 2017). *Drosophila* roles for Strip (variously with and without STRIPAK complex members) are equally diverse, with roles in cytoskeletal organisation (Bai et al., 2011), endocytosis (Sakuma et al., 2014), Ras-MAPK activation (Ashton-Beaucage et al., 2014), microtubule organisation (Sakuma et al., 2015), circadian rhythm (Andreazza et al., 2015), border cell migration (Madsen et al., 2015), Hippo signalling (Ribeiro et al., 2010; Sakuma et al., 2016) and autophagosome transport (Neisch et al., 2017).

This study represents the first in-depth exploration of Strip, Cka and TNF-JNK signalling during *Drosophila* spermatogenesis, and opens new avenues of investigation for these genes and pathways in other systems. However, roles for *Strip* and *Cka* have recently been identified in both the *Drosophila* adult testis and ovary. In the adult testis, a genome-wide RNAi screen for GSC regulators conducted using the ubiquitous *Actin-GAL4* driver revealed that *Cka* knockdown led to ectopic GSC-like cells in the adult testis, whereas *Strip* knockdown resulted in GSC loss (Liu et al., 2016); these results both reflect and contrast our own findings. In another study, researchers identified *Strip* in an RNAi screen for somatic lineage regulators of adult fertility, with *Strip* knockdown leading to total somatic cell loss (Fairchild et al., 2017). Various explanations exist for these phenotypic discrepancies: different driver choices, different RNAi lines or possibly subtle biological differences exist between the adult testis and larval gonad. Finally, in the adult ovary, *Strip* and *Cka* were isolated in an RNAi screen as being required for proper border cell migration (BCM) (Madsen et al., 2015), a process commonly used to model invasive cell behaviours (Montell, 2003;

Development (2019) 146, dev174292. doi:10.1242/dev.174292

Montell et al., 2012). As there is not thought to be a spermatogenesis process analogous to BCM, it is unlikely that parallels can be drawn between these data and our own, but it is interesting to note that JNK signalling plays a poorly understood role in BCM (Llense and Martín-Blanco, 2008; Mathieu et al., 2007).

A model for *Strip* regulation of JNK signalling in spermatogenesis

The highly conserved JNK signalling pathway has two broad roles: effecting stress response mechanisms or regulating cell shape changes. In either case, the pathway's kinase core of Hep and Bsk is retained, while upstream components can vary greatly (Ríos-Barrera and Riesgo-Escovar, 2013). We demonstrated that *Strip* and *Cka* negatively regulate the JNK signalling pathway, something previously demonstrated in the context of IMD signalling (Ashton-Beaucage et al., 2014; Bond and Foley, 2009). However, *imd* proved dispensable with regard to the activation of JNK signalling during spermatogenesis, while *Tak1*, *Traf6* and the *Drosophila* TNF *egr* are all necessary. This strongly suggests that JNK signalling is activated in the L3 male gonad via TNF signalling. However, only a low level of JNK signalling is observed in wild-type gonads – why, then, is the pathway strongly activated in *Strip*$^{jam/jam}$ gonads? Previous studies, along with this work, suggest that the ability of Strip/Cka to suppress JNK signalling likely proceeds via physical interactions with Hep and/or Bsk (Ashton-Beaucage et al., 2014; Bond and Foley, 2009; Chen et al., 2002). We propose that JNK signalling during spermatogenesis opposes proper somatic cell morphology and germline enclosure, and that JNK signalling is therefore normally downregulated to the low level we observed by the actions of Strip/Cka (Fig. 8, orange line). Therefore, activation of JNK signalling upon *Strip*/*Cka* mutation/knockdown leads to a concomitant disruption of proper somatic cell development.

As we determined *Strip* and *Cka* are necessary exclusively within the somatic lineage, why does defective germline differentiation and proliferation occur in *Strip*$^{jam/jam}$ gonads? Disruption of EGFR signalling in the testis prevents proper germline enclosure, and results in germline overproliferation phenotypes, similar to our own observations (Chen et al., 2013; Sarkar et al., 2007; Schulz et al., 2002). Furthermore, the somatic lineage is an important source of molecular signals for the germline lineage, and these can regulate behaviours such as differentiation (Leatherman and DiNardo, 2010; Singh et al., 2006; Wang et al., 2008). Thus, the germline phenotypes observed in *Strip*$^{jam/jam}$ gonads – ectopic Bam expression, supernumerary early cells, a lack of differentiation and ectopic proliferation – are likely to be secondary phenotypes, deriving from the defective somatic cell behaviours in *Strip* mutant gonads, and the resultant lack of proper cell-cell contact and enclosure of the germline lineage.

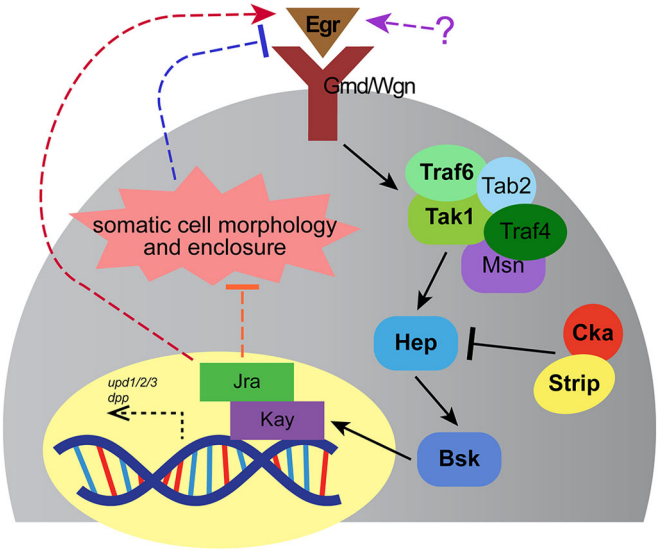

Fig. 8. A model for Strip, Cka and TNF-JNK signalling during spermatogenesis. JNK signalling, activated via TNF signalling, may negatively regulate the morphology of the somatic lineage, and its ability to properly enclose the germline lineage. Strip and Cka, in turn, negatively regulate JNK signalling, and allow for proper somatic cell behaviours and transcriptional regulation. The precise initiator of Egr upregulation after *Strip* mutation is unclear, but possibilities are represented by the coloured dotted lines. Bold indicates components examined in this study.

Links between *Strip*, JNK signalling and other processes

JNK signalling in spermatogenesis was essentially unstudied until recently, when it was found that knockdown of the endocytosis component, *Rab5*, in the adult testis somatic lineage, led to ectopic spermatogonial TA divisions, a process mediated by JNK and TGFβ signalling (Tang et al., 2017). Interestingly, Strip plays a role in endocytosis during *Drosophila* neurogenesis, contributing to early endosome organisation, clustering and fusion, processes in which Rab5 is integral (Sakuma et al., 2014). Exploring this link, we found that whilst endocytic components Rab5 (early endosomes) and Rab11 (recycling endosomes) were required in the gonad (Fig. S13A-B′), expression of constitutively active *Rab5* did not rescue *Strip*$^{jam/jam}$ gonad phenotypes (Fig. S13C-D′), in contrast to its rescue of *Strip* mutant olfactory projection neuron clones (Sakuma et al., 2014). Additionally, *Cka* is dispensable for neuronal morphogenesis (Sakuma et al., 2014), but crucial in spermatogenesis, as we have shown. Interestingly, *Rab11* knockdown leads to phenotypes highly reminiscent of *Strip* knockdown (Fig. S14A,A′) (Joti et al., 2011), but *Rab5* knockdown leads to ectopically TA spermatogonia (Fig. S14B,B′) (Tang et al., 2017). A more in-depth exploration of potential links between *Strip*, JNK signalling and endocytosis during spermatogenesis would be informative, particularly given the established links between JNK signalling and endocytosis (Froldi et al., 2010; Igaki et al., 2009; Robinson and Moberg, 2011).

An interesting question to arise from our research is: where does the Egr signal originate? TNF ligands in mammals are believed to be membrane-bound proteins, which can be cleaved, solubilised and then act in an autocrine or paracrine manner (Locksley et al., 2001; Smith et al., 1994). In *Drosophila*, it is unknown whether Egr behaves similarly or what the upstream regulators of its expression are, and the best-understood situation whereupon Egr expression is induced is after cell polarity loss (Igaki and Miura, 2014; Richardson and Portela, 2018). There, JNK signalling is activated in polarity-deficient cells via Egr secretion from various neighbouring cell types, and the mutant cells are eliminated via apoptosis. As we observed elevated cell death in *Strip*$^{jam/jam}$ gonads, a similar situation may be occurring – the disruptions to somatic cell morphology might lead to TNF-JNK-mediated cell death. This is an alternative to our previously suggested model, and places somatic cell morphology upstream of TNF-JNK signalling (Fig. 8, blue line). However, we observed no rescue of the *Strip*$^{jam/jam}$ mutant phenotype after blocking effector caspase activity via expression of *p35* in either the somatic or germline lineages (data not shown), suggesting JNK signalling plays a different role. JNK signalling has long been established as a cytoskeleton and cell shape regulator (Ríos-Barrera and Riesgo-Escovar, 2013; Rudrapatna et al., 2013), but it is not clear that this activity involves pathway activation via TNF signalling.

Development (2019) 146, dev174292. doi:10.1242/dev.174292

Another possible mechanism by which Egr expression could be induced in *Strip* mutant gonads is by TGFβ signalling – during spermatogenesis, TGFβ signalling is induced by JNK activation (Tang et al., 2017). Although it has long been known that *dpp*, a TGFβ signalling ligand, is a transcriptional target of JNK (Gavin-Smyth et al., 2013; Glise and Noselli, 1997; Hou et al., 1997; Mihaly et al., 2001; Riesgo-Escovar and Hafen, 1997; Takatsu et al., 2000; Zeitlinger et al., 1997), it has only recently been demonstrated that one of the targets of the TGFβ transcription factor, Mad, is *egr* (Dominguez et al., 2016; Gavin-Smyth et al., 2013), making TGFβ signalling an excellent candidate for explaining the source of the Egr expression observed in $Strip^{jam/jam}$ gonads in the form of a feedback loop. However, somatic lineage expression of RNAi against Mad [the efficacy of which was confirmed by pMad expression knockdown (data not shown)] did not rescue the $Strip^{jam/jam}$ phenotype (Fig. S14A-B′), suggesting that the upregulated TGFβ signalling we observed in $Strip^{jam/jam}$ gonads does not contribute to inducing *egr* expression. The possibility also remains that activated JNK signalling is itself driving Egr expression (Fig. 8, red line) or perhaps some unexamined pathway is involved (Fig. 8, purple line).

Finally, we considered a role for Jak-STAT signalling, a key regulator of spermatogenesis (Bausek, 2013), and a well-known target of JNK signalling, and which induces Unpaired-family expression in other tissues (Ammeux et al., 2016; Bunker et al., 2015; Jiang et al., 2009). We observed that Jak-STAT signalling was ectopically activated in $Strip^{jam/jam}$ gonads, as revealed by immunofluorescence for Stat92E (Fig. S14C-D′). *Stat92E* reporter co-expression with elevated levels of the JNK target Mmp1 was also observed in the somatic lineage (Fig. S14E-H″). However, somatic lineage knockdown of *Stat92E* did not rescue the $Strip^{jam/jam}$ phenotype, and only led to early germline cell loss (Fig. S14I-J′), suggesting that Jak-STAT signalling contributes to the established role of the somatic lineage in non-cell-autonomous regulation of germline lineage survival or proliferation (reviewed by Zoller and Schulz, 2012). Thus, although we were not able to dissect the precise upstream effectors of Egr expression, TNF-JNK signalling and how $Strip^{jam/jam}$ non-cell autonomously affects the germline lineage, our data collectively show the $Strip^{jam/jam}$ phenotype is highly complex, simultaneously displaying: activation of TNF-JNK signalling, activated TGFβ and Jak-STAT signalling, a loss-of-enclosure phenotype canonically indicative of – but seemingly not linked to – EGFR signalling disruption and increased proliferation alongside increased cell death. It seems likely that the $Strip^{jam/jam}$ phenotype is a combination of these different disruptions, which also potentially interact with or even effect each other.

Our study has identified novel roles for *Strip* and *Cka* in regulating TNF-JNK signalling during spermatogenesis. Furthermore, intriguing parallels exist between the roles for *Strip*, *Cka*, and TNF-JNK signalling in spermatogenesis, and their roles in other processes. Given the emerging relevance of the orthologues of *Strip* in human cancer (Madsen et al., 2015), further research into *Strip* using the powerful model systems available in *Drosophila* has the potential to provide important mechanistic insights into pathologically relevant roles of this gene.

MATERIALS AND METHODS

Fly stocks and husbandry

The Bloomington *Drosophila* Stock Center (BDSC) 3rd chromosome deficiency kit, *Df(3L)1227* (5410), *Df(3L)HR232* (3648), *Df(3L)Exel6094* (7573), *Df(3L)Exel6095* (7574), *Df(3L)Exel6096* (7575), *Df(3L)Exel6097* (7576), *Df(3L)BSC129* (9294), $UAS\text{-}rl^{SEM}$ (59006), $UAS\text{-}bsk^{DN}$ (9311), *UAS-luciferase RNAi* (31603), $UAS\text{-}Rab5^{Q88L}$ *YFP* (9774), *UAS-p35* (5072) and w^{1118} (3605, used as wild type) were all obtained from the BDSC. The *UAS-bsk RNAi* (v34138), *UAS-Ccm3 RNAi* (v106841), *UAS-Cka RNAi* (v106971), *UAS-Cka RNAi* (v35234), *UAS-Fgop2 RNAi* (v47389), *UAS-GckIII RNAi* (v49558), *UAS-GckIII RNAi* (v107158), *UAS-imd RNAi* (v101834), *UAS-Mad RNAi* (v12635), *UAS-Mob4 RNAi* (v110742), *UAS-msn RNAi* (v101517), *UAS-mts RNAi* (v35171), *UAS-Pp2A-29B RNAi* (v49671), *UAS-Pp2A-29B RNAi* (v49672), *UAS-Rab5 RNAi* (v34096), *UAS-Rab11 RNAi* (v108382), *UAS-Slmap RNAi* (v8199), *UAS-Stat92E RNAi* (v43866), *UAS-Strip RNAi* (v16211), *UAS-Strip RNAi* (v16212), *UAS-Tak1 RNAi* (v101357), *UAS-Traf6 RNAi* (v16125) and *UAS-Dcr-2* (v60009) stocks were all obtained from the Vienna Drosophila Resource Center (VDRC). The $Strip^{dogi}$, *Df(3L)tc-1* and $Strip\text{-}Myc^{2\text{-}38\text{-}4\text{-}1}$ stocks were gifts from Takahiro Chihara (Hiroshima University, Japan). The $UAS\text{-}Egfr^{DN}$, $UAS\text{-}Egfr^{\lambda}$, *UAS-GAL4;nanos-GAL4*, *Upd1-GAL4*, *C587-GAL4* and *tj-GAL4* stocks were gifts from Gary Hime (University of Melbourne, Australia). The *UAS-egr*, egr^{1} and egr^{3} stocks were gifts from Masayuki Miura (University of Tokyo, Japan). The $Mad^{1\text{-}2}$ and $Mad^{8\text{-}2}$ stocks were gifts from Donna Denton (University of South Australia, Australia). Other fly stocks used in this study were *10×Stat92E-GFP* (Bach et al., 2007) and *hsFLP;; Act>>GAL4, UAS-RFP / TM6B*. Flies were raised and all crosses undertaken within a controlled environmental incubator at 25°C (unless otherwise indicated) on a standard cornmeal, molasses and yeast medium. In all relevant crosses, *GAL4*-containing flies were virgin females. *UAS* construct-containing stocks that effected a modified gonad phenotype when expressed via *C587-GAL4* were checked for their gonad phenotype independently of *GAL4* expression, and were all found to be wild type in appearance.

Generation of mutant stocks for the forward genetic screen

Late-larval and early-pupal lethal stocks were generated via administration of ethyl methanesulfonate (EMS) treatment (5 mM) to isogenised *FRT82B* flies. Mutagenised stocks were maintained using the balancer chromosome, $TM6B, Tb^{1}, Antp^{Hu}$.

Immunofluorescence, imaging and antibodies

L3 male gonads were dissected in 1× phosphate-buffered saline (PBS) (Amresco, E703) and fixed for 15 min in 4% paraformaldehyde (PFA) (ProSciTech, C005; Alfa Aesar, 43368) in PBS with 0.1% Triton X-100 (PBST). During the screening process, gonads were then washed in PBST and mounted in ProLong Gold Antifade Reagent with DAPI (Molecular Probes, P36935), examined using a Nikon Eclipse Ti Inverted Microscope System and imaged using NIS-Elements Imaging Software (Nikon Instruments). During other experiments, gonads were washed in PBST and blocked in PBST containing 5% normal horse serum (NHS) (Sigma-Aldrich, H0146) for 1 h at room temperature, then incubated overnight at 4°C with primary antibodies diluted in 5% NHS in PBST. Tissues were then washed in PBST and incubated in secondary antibody diluted in 5% NHS in PBST at room temperature for 1.5 h, then washed again in PBST and mounted using ProLong Gold Antifade Reagent with DAPI. Samples were imaged using a Zeiss LSM 510 or Zeiss LSM 780 laser scanning confocal microscope, and imaged using Zen 2012 software (Carl Zeiss). Primary antibodies used were: mouse anti-BrdU (1:200, #5292), rabbit anti-Cleaved Caspase-3 (1:5000, #661), anti-Myc tag (1:4000, 2276), mouse anti-phospho Histone H3 (1:1000, 9706), rabbit anti-phospho-p44/42 MAPK (Erk1/2) (1:200, 4370), rabbit anti-phospho Smad 1/5 (1:100, 13820) (all from Cell Signaling Technology); mouse anti-Hts (1:20, 1B1), mouse anti-Discs large 1 (1:50, 4F3), mouse anti-Bam (1:25), mouse anti-Armadillo (1:10, N27A1), mouse anti-Eyes absent (1:100, 10H6), mouse anti-Fas3 (1:25, 7G10), mouse anti-Mmp1 (1:50, 5H7B11, 3B8D12 and 3A6B4 mixed in a 1:1:1 cocktail) (all from the Developmental Studies Hybridoma Bank); goat anti-Vasa (1:100, sc-26877) (Santa Cruz Biotechnology); rabbit anti-ACTIVE JNK pAb (1:500, V793A) (Promega); rabbit anti-Stat92E (1:1000) (a gift from Erika Bach, New York University, USA); rabbit anti-Zn finger homeodomain 1 (1:5000) (a gift from Ruth Lehmann, New York University, USA); rat anti-Matotopetli (1:500) (a gift from Helen White-Cooper, Cardiff University, UK); guinea pig anti-Traffic jam (1:5000) (a gift from Dorothea Godt, University of Toronto, Canada); rabbit anti-Eiger (1:250) (a gift from Masayuki Miura, University of Tokyo, Japan); mouse anti-Nimrod C1

Development (2019) 146, dev174292. doi:10.1242/dev.174292

(1:500) (a gift from István Andó, Hungarian Academy of Sciences). Alexa Fluor secondary antibodies (A-11055, A-11058, A-21447, A-11073, A-21202, A-21203, A-31571, A-21206, A-21207, A-31573, A-21208 and A-21209, Molecular Probes) were used at dilutions of 1:500.

BrdU incorporation and TUNEL assays

Prior to fixation, gonads were incubated in 0.326 mM BrdU (Sigma-Aldrich, B5002) for 1 h at room temperature. After fixation for 15 min in 4% PFA, tissues were washed in PBST, treated with 50 U/ml DNase I (Invitrogen, 18068-015) for 45 min at 37°C, and the reaction halted with 2 µl EDTA (25 mM) (Amresco, 0322). TUNEL assays were performed using a Click-iT Plus TUNEL Assay kit (Molecular Probes, C16019).

Quantifications

To quantify M-phase cells, overlapping *z*-sections were taken through whole gonads stained for pHis3, Zfh1 and Vasa. Using Zen 2012 software, the numbers of proliferating germline cells (co-expressing pHis3 and Vasa) and somatic cells (co-expressing pHis3 and Zfh1) were quantified. To generate Fig. 3E, synchronously proliferating germline cells within spermatogonia and spermatocytes were counted as single proliferating cells, and the significance was assessed using Student's *t*-test. To generate Fig. 3F, proliferating somatic cells were ignored, and the number of each type of germline cell undergoing proliferation was judged by appearance and the proximity of pHis3 stains. To quantify gonad sizes, their area was measured using Fiji (Schindelin et al., 2012) at the *z*-section of their largest circumference. Data were analysed using Student's *t*-test and visualised using GraphPad Prism 7.

Venus-tagged full-length *Strip* construct and transgenic fly generation

Full-length *Strip* (isoform A) open reading frame (ORF) sequence was amplified from the expressed sequence tag (EST) AT20596 [*Drosophila* Genomics Research Center (DGRC), 1035472] via PCR using *Pfu* DNA polymerase (Promega, #M7741) and the following primers: 5′-CACCATG-ATGCTCACATCCATAAACAACTC-3′ (forward); and 5′-AGGGCGTCC-CAGTCGGTC-3′ (reverse).

The Strip ORF was cloned into a pTVW vector (DGRC, 1091) using a standard Gateway Technology method (Life Technologies, #12535-019). The pTVW-Strip expression clone was purified using a Purelink HiPure Plasmid Filter Midiprep Kit (Life Technologies, K210014) and used to create transgenic fly stocks by BestGene.

Co-immunoprecipitation and western blotting

L3 carcasses, with the gut removed, were washed and dissected in 1× PBS and homogenised in NETN lysis buffer (cshprotocols.cshlp.org/content/2009/1/pdb.rec11595.full) with added PMSF proteinase inhibitor (Amresco, M145) and a phosphatase inhibitor cocktail (Sigma-Aldrich, P5726). Sample lysate protein concentration was quantified using a DC Protein Assay kit (BioRad, 500-0112). Some lysate was set aside and used as the positive control (input).

For co-immunoprecipitation experiments, primary antibodies were added to sample lysates and incubated overnight at 4°C. Primary antibodies used were: rat anti-Strip (1:100) (a gift from Takahiro Chihara, Hiroshima University, Japan) and rabbit anti-Cka (1:1000) (a gift from Wei Du, The University of Chicago, USA). Negative control samples underwent identical treatments, but without incubation with primary antibodies. Samples were incubated for 4 h with Protein G Sepharose 4 Fast Flow beads (GE Healthcare, 17-0618-01) then washed with TBST.

Samples were boiled for 5 min in 1× Laemmli SDS buffer, and loaded on a 4-15% Mini-PROTEAN TGX Precast Protein Gels (BioRad, 456-1084). Samples loaded were of equal protein quantity (1×), alongside an additional experimental quantity (2×). Gels were run at 200 V and Precision Plus Protein WesternC Standards (Bio-Rad, 161-0376) was used as a ladder. Blotting was performed with a Trans-Blot Turbo Transfer pack (Bio-Rad, 170-4156, 170-4158). Membranes were blocked in 5% skim milk blocking solution and washed with TBST. Primary antibodies used were: mouse anti-β-Tubulin (1:200) (DSHB); rat anti-Strip (1:200) (a gift from Takahiro Chihara); rabbit anti-Cka (1:1500) (a gift from Wei Du); rabbit anti-Hep (1:250, ab1957) (a gift from Julian Ng, University of Cambridge, UK). Secondary antibodies used were: anti-rat HRP (1:1000, P0450), anti-mouse HRP (1:1000, P0447) and anti-rabbit HRP (1:2000, P0448) (all from Dako); and anti-rabbit HRP, light chain specific (1:10000, 211-032-171) (Jackson ImmunoResearch Laboratories). Blots were visualised using the Clarity Western ECL Substrate kit (BioRad, 170-5060) or the Amersham ECL Western Blot Detection Reagents kit (GE Healthcare, RPN220), and imaged using a GelDoc XRS+ system (BioRad).

Strip-Myc stock generation via CRISPR/Cas9

We aimed to generate a stock containing endogenous Strip tagged at the C terminus with 3×Myc epitope tag sequences via CRISPR/Cas9 gene editing. To generate the guide RNA plasmid, DNA oligos (5′-GTCGACCGACTG-GGACGCCCTCT-3′ and 5′-AAACAGAGGGCGTCCCAGTCGGT-3′) were hybridised and subcloned into *Bbs*I-digested *pCFD3-dU6:3gRNA* plasmid (Addgene, 49410) (a gift from Simon Bullock, University of Cambridge, UK) (Fig. S6A-C). The homology-directed repair (HDR) donor plasmid, consisting of a 3×Myc tag and 500 bp homology arms, was synthesised by GenScript (Fig. S6D,E). Microinjection of flies, stock generation and PCR screening were performed by WellGenetics. Transgenic flies expressing the guide RNA (*y*^{2}, *cho*^{2}, *v*^{1}*; pCFD3:U6:3-3×Myc-Strip@attP40/CyO*) were generated and crossed with *Cas9*-expressing flies, and ∼200 progeny were injected with the HDR donor plasmid. Following PCR screening (using the primers 5′-TCTTCTGAGATGAGTTTTTGTTC-G-3′ and 5′-CTTACCCACTCGGACTTTGC-3′) and DNA sequencing (using the primer 5′-ACCTCAAGCCAAGTGTCGTT-3′), eight stocks possessing *Strip::3×Myc* (*w*^{1118}*;; Strip::3×Myc / TM6B*) were generated.

Quantitative reverse transcription PCR

RNAi lines were crossed to *hsFLP;; Act>>GAL4, UAS-RFP/TM6B* and raised at 25°C, and heat-shocked at 37°C for 1 h as first-instar larvae to activate transgene expression. Tissue for RNA extraction (n>10 animals per genotype) was acquired from adults for the cross to the RNAi line against *imd*, and from pupae for the crosses to RNAi lines against *Fgop2*, *GckIII*, *Mob4*, *msn* and *Slmap*, as these latter crosses were lethal at the pupal stage. Tissue from both adults and pupae was obtained for the control crosses to the RNAi line against *luciferase*. RNA was extracted using an RNeasy Mini Kit (QIAGEN, 74104). DNA digestion was performed using an ezDNase kit (Invitrogen, 11766051). Synthesis of cDNA was performed using a SuperScript III First-Strand Synthesis kit (Invitrogen, 18080-051). RT-qPCR was performed using Power SYBR Green PCR Master Mix (Applied Biosystems, 4367659) on a CFX384 Touch Real-Time PCR Detection System (BioRad). Quantification cycle (Cq) values were obtained using BioRad CFX Manager software (v3.1). The data were normalised to expression of the housekeeping gene *Gapdh2*. The primer sequences used are as follows: *Fgop2*, forward 5′-TACCCGCACCGAACTGCC-3′ and reverse 5′-AATCTGGCCCACGGATAGGT-3′; *GckIII*, forward 5′-CGAA-GCCGTAGCAAATTCCG-3′ and reverse 5′-ATGTCTGCTCCAGCGTTT-CA-3′; *Mob4*, forward 5′-ACTTCCCTAGCAGGGTGTCC-3′ and reverse 5′-CACAGATACGTCTCGGCCTC-3′; *msn*, forward 5′-CCCGCTTTTGG-TCGATCTCA-3′ and reverse: 5′-TGCACCCTGAGTATGCTTGG-3′; *Slmap*, forward 5′-GAACTCTGCGATGTGTTGGC-3′ and reverse: 5′-TG-GCAGTCAACTGGTACGTT-3′; *imd*, forward 5′-GGGATCTTGGCATG-TCGGAA-3′ and reverse 5′-ACAGCTGGTATATCACCTCTCTA-3′; *Gapdh2*, forward 5′-GCAAGCAAGCCGATAGATAAACA-3′ and reverse 5′-CGTTGGCGCCCTTATCAATG-3′.

Acknowledgements

We thank Peter Lock and the LIMS Bioimaging Facility for microscopy equipment and technical support. We thank Keng Chen for his role in generating the EMS mutant collection used in our screen. We thank the Australian *Drosophila* research community, the BDSC and the VDRC for providing fly stocks, and OzDros for stock importation services. We also thank Linda Parsons, Jan Manent, Peter Burke, Molly Buntine, Sachini Arachchilage, Marta Portela, Kirsten Allan, Monica Ivanyi and Alex Lowdin for suggestions and general experimental assistance. The *Drosophila* Genomics Resource Center is supported by a National Institutes of Health grant (2P40OD010949). The Developmental Studies Hybridoma Bank was created by the National Institute of Child Health and Human Development of the National Institutes of Health and is based at The University of Iowa. Indicated

transgenic fly stocks were obtained from the Vienna Drosophila Resource Center (Dietzl et al., 2007).

Competing interests
The authors declare no competing or financial interests.

Author contributions
Conceptualization: J.E.L.M., S.T.D., H.W., A.H.H., H.E.R., W.G.S.; Methodology: J.E.L.M., S.T.D., A.L.H., H.W., H.E.R., W.G.S.; Validation: J.E.L.M., S.T.D., A.L.H., W.G.S.; Formal analysis: J.E.L.M., W.G.S.; Investigation: J.E.L.M., S.T.D., A.L.H., W.G.S.; Resources: J.E.L.M., S.T.D., A.L.H., H.W., H.E.R., W.G.S.; Writing - original draft: J.E.L.M.; Writing - review & editing: J.E.L.M., S.T.D., H.E.R., W.G.S.; Visualization: J.E.L.M., S.T.D.; Supervision: H.W., A.H.H., H.E.R., W.G.S.; Project administration: J.E.L.M., H.W., A.H.H., H.E.R., W.G.S.; Funding acquisition: H.W., H.E.R., W.G.S.

Funding
OzDros is supported by a National Health and Medical Research Council enabling grant (418033). J.E.L.M. was supported by a La Trobe University David Myers scholarship and an Australian Research Council Discovery grant (DP170102549 to H.E.R.). S.T.D. was supported by a La Trobe University Postgraduate Research Scholarship. H.E.R. was supported by a National Health and Medical Research Council fellowship (1020056) and funds from the La Trobe Institute for Molecular Science and La Trobe University. H.W. was supported by the Singapore National Medical Research Council (NMRC/CBRG/0082/2015). W.G.S. was supported by a National Health and Medical Research Council Peter Doherty Australian Biomedical Fellowship (520307). A.H.H. was supported by a National Health and Medical Research Council grant (GNT0606691).

Supplementary information
Supplementary information available online at
http://dev.biologists.org/lookup/doi/10.1242/dev.174292.supplemental

References
Ammeux, N., Housden, B. E., Georgiadis, A., Hu, Y. and Perrimon, N. (2016). Mapping signaling pathway cross-talk in *Drosophila* cells. *Proc. Natl. Acad. Sci. USA* **113**, 9940-9945. doi:10.1073/pnas.1610432113

Andersen, D. S., Colombani, J., Palmerini, V., Chakrabandhu, K., Boone, E., Röthlisberger, M., Toggweiler, J., Basler, K., Mapelli, M., Hueber, A.-O. et al. (2015). The *Drosophila* TNF receptor Grindelwald couples loss of cell polarity and neoplastic growth. *Nature* **522**, 482-486. doi:10.1038/nature14298

Andreazza, S., Bouleau, S., Martin, B., Lamouroux, A., Ponien, P., Papin, C., Chélot, E., Jacquet, E. and Rouyer, F. (2015). Daytime CLOCK dephosphorylation is controlled by STRIPAK complexes in *Drosophila*. *Cell Rep.* **11**, 1266-1279. doi:10.1016/j.celrep.2015.04.033

Ashton-Beaucage, D., Udell, C. M., Gendron, P., Sahmi, M., Lefrançois, M., Baril, C., Guenier, A.-S., Duchaine, J., Lamarre, D., Lemieux, S. et al. (2014). A functional screen reveals an extensive layer of transcriptional and splicing control underlying RAS/MAPK signaling in *Drosophila*. *PLoS Biol.* **12**, 1-22. doi:10.1371/journal.pbio.1001809

Bach, E. A., Ekas, L. A., Ayala-Camargo, A., Flaherty, M. S., Lee, H., Perrimon, N. and Baeg, G.-H. (2007). GFP reporters detect the activation of the *Drosophila* JAK/STAT pathway *in vivo*. *Gene Expr. Patterns* **7**, 323-331. doi:10.1016/j.modgep.2006.08.003

Bai, S. W., Herrera-Abreu, M. T., Rohn, J. L., Racine, V., Tajadura, V., Suryavanshi, N., Bechtel, S., Wiemann, S., Baum, B. and Ridley, A. J. (2011). Identification and characterization of a set of conserved and new regulators of cytoskeletal organization, cell morphology and migration. *BMC Biol.* **9**, 1-18. doi:10.1186/1741-7007-9-1

Batlle, E. and Clevers, H. (2017). Cancer stem cells revisited. *Nat. Med.* **23**, 1124-1134. doi:10.1038/nm.4409

Bausek, N. (2013). JAK-STAT signaling in stem cells and their niches in *Drosophila*. *JAK-STAT* **2**, 1-11. doi:10.4161/jkst.25686

Bazzi, H., Soroka, E., Alcorn, H. L. and Anderson, K. V. (2017). STRIP1, a core component of STRIPAK complexes, is essential for normal mesoderm migration in the mouse embryo. *Proc. Natl Acad. Sci. USA* **114**, 10928-10936. doi:10.1073/pnas.1713535114

Bond, D. and Foley, E. (2009). A quantitative RNAi screen for JNK modifiers identifies Pvr as a novel regulator of *Drosophila* immune signaling. *PLoS Pathog.* **5**, 1-13. doi:10.1371/journal.ppat.1000655

Bunker, B. D., Nellimoottil, T. T., Boileau, R. M., Classen, A. K. and Bilder, D. (2015). The transcriptional response to tumorigenic polarity loss in *Drosophila*. *eLife* **4**, 1-19. doi:10.7554/eLife.03189

Cabarcas, S. M., Mathews, L. A. and Farrar, W. L. (2011). The cancer stem cell niche-there goes the neighborhood? *Int. J. Cancer* **129**, 2315-2327. doi:10.1002/ijc.26312

Castrillon, D. H., Gonczy, P., Alexander, S., Rawson, R., Eberhart, C. G., Viswanathan, S., DiNardo, S. and Wasserman, S. A. (1993). Toward a molecular genetic analysis of spermatogenesis in *Drosophila melanogaster*: characterization of male-sterile mutants generated by single P element mutagenesis. *Genetics* **135**, 489-505.

Chen, H.-W., Marinissen, M. J., Oh, S.-W., Chen, X., Melnick, M., Perrimon, N., Gutkind, J. S. and Hou, S. X. (2002). CKA, a novel multidomain protein, regulates the JUN N-terminal kinase signal transduction pathway in *Drosophila*. *Mol. Cell. Biol.* **22**, 1792-1803. doi:10.1128/MCB.22.6.1792-1803.2002

Chen, H., Chen, X. and Zheng, Y. (2013). The nuclear lamina regulates germline stem cell niche organization via modulation of EGFR signaling. *Cell Stem Cell* **13**, 73-86. doi:10.1016/j.stem.2013.05.003

Dalerba, P., Cho, R. W. and Clarke, M. F. (2007). Cancer stem cells: models and concepts. *Annu. Rev. Med.* **58**, 267-284. doi:10.1146/annurev.med.58.062105.204854

Demarco, R. S., Eikenes, Å. H., Haglund, K. and Jones, D. L. (2014). Investigating spermatogenesis in *Drosophila melanogaster*. *Methods* **68**, 218-227. doi:10.1016/j.ymeth.2014.04.020

Dietzl, G., Chen, D., Schnorrer, F., Su, K.-C., Barinova, Y., Fellner, M., Gasser, B., Kinsey, K., Oppel, S., Scheiblauer, S. et al. (2007). A genome-wide transgenic RNAi library for conditional gene inactivation in *Drosophila*. *Nature* **448**, 151-156. doi:10.1038/nature05954

Dominado, N., La Marca, J. E., Siddall, N. A., Heaney, J., Tran, M., Cai, Y., Yu, F., Wang, H., Somers, W. G., Quinn, L. M. et al. (2016). Rbf regulates *Drosophila* spermatogenesis via control of somatic stem and progenitor cell fate in the larval testis. *Stem Cell Rep.* **7**, 1152-1163. doi:10.1016/j.stemcr.2016.11.007

Dominguez, C., Zuñiga, A., Hanna, P., Hodar, C., Gonzalez, M. and Cambiazo, V. (2016). Target genes of Dpp/BMP signaling pathway revealed by transcriptome profiling in the early *D. melanogaster* embryo. *Gene* **591**, 191-200. doi:10.1016/j.gene.2016.07.015

Fabrizio, J. J., Boyle, M. and DiNardo, S. (2003). A somatic role for *eyes absent* (*eya*) and *sine oculis* (*so*) in *Drosophila* spermatocyte development. *Dev. Biol.* **258**, 117-128. doi:10.1016/S0012-1606(03)00127-1

Fairchild, M. J., Islam, F. and Tanentzapf, G. (2017). Identification of genetic networks that act in the somatic cells of the testis to mediate the developmental program of spermatogenesis. *PLoS Genet.* **13**, e1007026. doi:10.1371/journal.pgen.1007026

Fan, Y. and Bergmann, A. (2010). The cleaved-Caspase-3 antibody is a marker of Caspase-9-like DRONC activity in *Drosophila*. *Cell Death Differ.* **17**, 534-539. doi:10.1038/cdd.2009.185

Fogarty, C. E., Diwanji, N., Lindblad, J. L., Tare, M., Amcheslavsky, A., Makhijani, K., Brückner, K., Fan, Y. and Bergmann, A. (2016). Extracellular reactive oxygen species drive apoptosis-induced proliferation via *Drosophila* macrophages. *Curr. Biol.* **26**, 575-584. doi:10.1016/j.cub.2015.12.064

Friedman, A. and Perrimon, N. (2006). A functional RNAi screen for regulators of receptor tyrosine kinase and ERK signalling. *Nature* **444**, 230-234. doi:10.1038/nature05280

Froldi, F., Ziosi, M., Garoia, F., Pession, A., Grzeschik, N. A., Bellosta, P., Strand, D., Richardson, H. E., Pession, A. and Grifoni, D. (2010). The *lethal giant larvae* tumour suppressor mutation requires dMyc oncoprotein to promote clonal malignancy. *BMC Biol.* **8**, 1-16. doi:10.1186/1741-7007-8-33

Frost, A., Elgort, M. G., Brandman, O., Ives, C., Collins, S. R., Miller-Vedam, L., Weibezahn, J., Hein, M. Y., Poser, I., Mann, M. et al. (2012). Functional repurposing revealed by comparing *S. pombe* and *S. cerevisiae* genetic interactions. *Cell* **149**, 1339-1352. doi:10.1016/j.cell.2012.04.028

Fuller, M. T. (1993). Spermatogenesis. In *The Development of Drosophila Melanogaster* (ed. M. Bate and A. Martinez Arias), pp. 71-147. Cold Spring Harbor, New York, United States of America: Cold Spring Harbor Laboratory Press.

Gavin-Smyth, J., Wang, Y.-C., Butler, I. and Ferguson, E. L. (2013). A genetic network conferring canalization to a bistable patterning system in *Drosophila*. *Curr. Biol.* **23**, 2296-2302. doi:10.1016/j.cub.2013.09.055

Glise, B. and Noselli, S. (1997). Coupling of Jun amino-terminal kinase and Decapentaplegic signaling pathways in *Drosophila* morphogenesis. *Genes Dev.* **11**, 1738-1747. doi:10.1101/gad.11.13.1738

Gönczy, P., Matunis, E. and DiNardo, S. (1997). *bag-of-marbles* and *benign gonial cell neoplasm* act in the germline to restrict proliferation during *Drosophila* spermatogenesis. *Development* **124**, 4361-4371.

Goudreault, M., D'Ambrosio, L. M., Kean, M. J., Mullin, M. J., Larsen, B. G., Sanchez, A., Chaudhry, S., Chen, G. I., Sicheri, F., Nesvizhskii, A. I. et al. (2009). A PP2A phosphatase high density interaction network identifies a novel striatin-interacting phosphatase and kinase complex linked to the cerebral cavernous malformation 3 (CCM3) protein. *Mol. Cell. Proteomics* **8**, 157-171. doi:10.1074/mcp.M800266-MCP200

Greenspan, L. J., de Cuevas, M. and Matunis, E. (2015). Genetics of gonadal stem cell renewal. *Annu. Rev. Cell Dev. Biol.* **31**, 291-315. doi:10.1146/annurev-cellbio-100913-013344

Guruharsha, K. G., Rual, J.-F., Zhai, B., Mintseris, J., Vaidya, P., Vaidya, N., Beekman, C., Wong, C., Rhee, D. Y., Cenaj, O. et al. (2011). A protein complex network of *Drosophila melanogaster*. *Cell* **147**, 690-703. doi:10.1016/j.cell.2011.08.047

Hackstein, J. H. (1991). Spermatogenesis in *Drosophila*. A genetic approach to cellular and subcellular differentiation. *Eur. J. Cell Biol.* **56**, 151-169.
Hardy, R. W., Tokuyasu, K. T., Lindsley, D. L. and Garavito, M. (1979). The germinal proliferation center in the testis of *Drosophila melanogaster*. *J. Ultrastruct. Res.* **69**, 180-190. doi:10.1016/S0022-5320(79)90108-4
Hay, B., Ackerman, L., Barbel, S., Jan, L. Y. and Jan, Y. N. (1988). Identification of a component of *Drosophila* polar granules. *Development* **103**, 625-640.
Hoffmann, J. A. (2003). The immune response of *Drosophila*. *Nature* **426**, 33-38. doi:10.1038/nature02021
Horn, T., Sandmann, T., Fischer, B., Axelsson, E., Huber, W. and Boutros, M. (2011). Mapping of signaling networks through synthetic genetic interaction analysis by RNAi. *Nat. Methods* **8**, 341-346. doi:10.1038/nmeth.1581
Hou, X. S., Goldstein, E. S. and Perrimon, N. (1997). *Drosophila* Jun relays the Jun amino-terminal kinase signal transduction pathway to the Decapentaplegic signal transduction pathway in regulating epithelial cell sheet movement. *Genes Dev.* 11, 1728-1737. doi:10.1101/gad.11.13.1728
Hudson, A. G., Parrott, B. B., Qian, Y. and Schulz, C. (2013). A temporal signature of epidermal growth factor signaling regulates the differentiation of germline cells in testes of *Drosophila melanogaster*. *PLoS ONE* **8**, 1-12. doi:10.1371/journal.pone.0070678
Hwang, J. and Pallas, D. C. (2014). STRIPAK complexes: structure, biological function, and involvement in human diseases. *Int. J. Biochem. Cell Biol.* **47**, 118-148. doi:10.1016/j.biocel.2013.11.021
Igaki, T. and Miura, M. (2014). The *Drosophila* TNF ortholog Eiger: emerging physiological roles and evolution of the TNF system. *Semin. Immunol.* **26**, 267-274. doi:10.1016/j.smim.2014.05.003
Igaki, T., Kanda, H., Yamamoto-Goto, Y., Kanuka, H., Kuranaga, E., Aigaki, T. and Miura, M. (2002). Eiger, a TNF superfamily ligand that triggers the *Drosophila* JNK pathway. *EMBO J.* **21**, 3009-3018. doi:10.1093/emboj/cdf306
Igaki, T., Pastor-Pareja, J. C., Aonuma, H., Miura, M. and Xu, T. (2009). Intrinsic tumor suppression and epithelial maintenance by endocytic activation of Eiger/TNF signaling in *Drosophila*. *Dev. Cell* **16**, 458-465. doi:10.1016/j.devcel.2009.01.002
Insco, M. L., Leon, A., Tam, C. H., McKearin, D. M. and Fuller, M. T. (2009). Accumulation of a differentiation regulator specifies transit amplifying division number in an adult stem cell lineage. *Proc. Natl Acad. Sci. USA* **106**, 22311-22316. doi:10.1073/pnas.0912454106
Jiang, H., Patel, P. H., Kohlmaier, A., Grenley, M. O., McEwen, D. G. and Edgar, B. A. (2009). Cytokine/Jak/Stat signaling mediates regeneration and homeostasis in the *Drosophila* midgut. *Cell* **137**, 1343-1355. doi:10.1016/j.cell.2009.05.014
Joti, P., Ghosh-Roy, A. and Ray, K. (2011). Dynein light chain 1 functions in somatic cyst cells regulate spermatogonial divisions in *Drosophila*. *Sci. Rep.* **1**, 1-9. doi:10.1038/srep00173
Kaneko, T. and Silverman, N. (2005). Bacterial recognition and signalling by the *Drosophila* IMD pathway. *Cell. Microbiol.* **7**, 461-469. doi:10.1111/j.1462-5822.2005.00504.x
Kawase, E., Wong, M. D., Ding, B. C. and Xie, T. (2004). Gbb/Bmp signaling is essential for maintaining germline stem cells and for repressing *bam* transcription in the *Drosophila* testis. *Development* **131**, 1365-1375. doi:10.1242/dev.01025
Kearse, M., Moir, R., Wilson, A., Stones-Havas, S., Cheung, M., Sturrock, S., Buxton, S., Cooper, A., Markowitz, S., Duran, C. et al. (2012). Geneious basic: an integrated and extendable desktop software platform for the organization and analysis of sequence data. *Bioinformatics* **28**, 1647-1649. doi:10.1093/bioinformatics/bts199
Kemp, H. A. and Sprague, G. F.Jr (2003). Far3 and five interacting proteins prevent premature recovery from pheromone arrest in the budding yeast *Saccharomyces cerevisiae*. *Mol. Cell. Biol.* **23**, 1750-1763. doi:10.1128/MCB.23.5.1750-1763.2003
Kiger, A. A., White-Cooper, H. and Fuller, M. T. (2000). Somatic support cells restrict germline stem cell self-renewal and promote differentiation. *Nature* **407**, 750-754. doi:10.1038/35037606
Kim, K., Lee, Y. S., Harris, D., Nakahara, K. and Carthew, R. W. (2006). The RNAi pathway initiated by Dicer-2 in *Drosophila*. *Cold Spring Harbor Symp. Quant. Biol.* **71**, 39-44. doi:10.1101/sqb.2006.71.008
Kück, U., Beier, A. M. and Teichert, I. (2016). The composition and function of the striatin-interacting phosphatases and kinases (STRIPAK) complex in fungi. *Fungal Genet. Biol.* **90**, 31-38. doi:10.1016/j.fgb.2015.10.001
La Marca, J. E. and Somers, W. G. (2014). The *Drosophila* gonads: models for stem cell proliferation, self-renewal, and differentiation. *AIMS Genetics* **1**, 55-80. doi:10.3934/genet.2014.1.55
Leatherman, J. L. and DiNardo, S. (2008). *Zfh-1* controls somatic stem cell self-renewal in the *Drosophila* testis and nonautonomously influences germline stem cell self-renewal. *Cell Stem Cell* **3**, 44-54. doi:10.1016/j.stem.2008.05.001
Leatherman, J. L. and DiNardo, S. (2010). Germline self-renewal requires cyst stem cells and stat regulates niche adhesion in *Drosophila* testes. *Nat. Cell Biol.* **12**, 806-811. doi:10.1038/ncb2086
Li, L. and Xie, T. (2005). Stem cell niche: structure and function. *Annu. Rev. Cell Dev. Biol.* **21**, 605-631. doi:10.1146/annurev.cellbio.21.012704.131525
Li, M. A., Alls, J. D., Avancini, R. M., Koo, K. and Godt, D. (2003). The large Maf factor traffic jam controls gonad morphogenesis in *Drosophila*. *Nat. Cell Biol.* **5**, 994-1000. doi:10.1038/ncb1058
Lighthouse, D. V., Buszczak, M. and Spradling, A. C. (2008). New components of the *Drosophila* fusome suggest it plays novel roles in signaling and transport. *Dev. Biol.* **317**, 59-71. doi:10.1016/j.ydbio.2008.02.009
Lin, H., Yue, L. and Spradling, A. C. (1994). The *Drosophila* fusome, a germline-specific organelle, contains membrane skeletal proteins and functions in cyst formation. *Development* **120**, 947-956.
Lisa-Santamaría, P., Jiménez, A. and Revuelta, J. L. (2012). The protein factor-arrest 11 (Far11) is essential for the toxicity of human caspase-10 in yeast and participates in the regulation of autophagy and the DNA damage signaling. *J. Biol. Chem.* **287**, 29636-29647. doi:10.1074/jbc.M112.344192
Liu, Y., Ge, Q., Chan, B., Liu, H., Singh, S. R., Manley, J., Lee, J., Weideman, A. M., Hou, G. and Hou, S. X. (2016). Whole-animal genome-wide RNAi screen identifies networks regulating male germline stem cells in *Drosophila*. *Nat. Commun.* **7**, 1-11. doi:10.1038/ncomms12149
Llense, F. and Martín-Blanco, E. (2008). JNK signaling controls border cell cluster integrity and collective cell migration. *Curr. Biol.* **18**, 538-544. doi:10.1016/j.cub.2008.03.029
Locksley, R. M., Killeen, N. and Lenardo, M. J. (2001). The TNF and TNF receptor superfamilies: integrating mammalian biology. *Cell* **104**, 487-501. doi:10.1016/S0092-8674(01)00237-9
Madsen, C. D., Hooper, S., Tozluoglu, M., Bruckbauer, A., Fletcher, G., Erler, J. T., Bates, P. A., Thompson, B. and Sahai, E. (2015). STRIPAK components determine mode of cancer cell migration and metastasis. *Nat. Cell Biol.* **17**, 68-80. doi:10.1038/ncb3083
Maheshwari, R., Pushpa, K. and Subramaniam, K. (2016). A role for post-transcriptional control of endoplasmic reticulum dynamics and function in *C. elegans* germline stem cell maintenance. *Development* **143**, 3097-3108. doi:10.1242/dev.134056
Mathieu, J., Sung, H.-H., Pugieux, C., Soetaert, J. and Rorth, P. (2007). A sensitized PiggyBac-based screen for regulators of border cell migration in *Drosophila*. *Genetics* **176**, 1579-1590. doi:10.1534/genetics.107.071282
Matunis, E., Tran, J., Gonczy, P., Caldwell, K. and DiNardo, S. (1997). Punt and schnurri regulate a somatically derived signal that restricts proliferation of committed progenitors in the germline. *Development* **124**, 4383-4391.
Matunis, E. L., Stine, R. R. and de Cuevas, M. (2012). Recent advances in *Drosophila* male germline stem cell biology. *Spermatogenesis* **2**, 137-144. doi:10.4161/spmg.21763
Mihaly, J., Kockel, L., Gaengel, K., Weber, U., Bohmann, D. and Mlodzik, M. (2001). The role of the *Drosophila* TAK homologue dTAK during development. *Mech. Dev.* **102**, 67-79. doi:10.1016/S0925-4773(01)00285-4
Montell, D. J. (2003). Border-cell migration: the race is on. *Nat. Rev. Mol. Cell Biol.* **4**, 13-24. doi:10.1038/nrm1006
Montell, D. J., Yoon, W. H. and Starz-Gaiano, M. (2012). Group choreography: mechanisms orchestrating the collective movement of border cells. *Nat. Rev. Mol. Cell Biol.* **13**, 631-645. doi:10.1038/nrm3433
Nagai, T., Ibata, K., Park, E. S., Kubota, M., Mikoshiba, K. and Miyawaki, A. (2002). A variant of yellow fluorescent protein with fast and efficient maturation for cell-biological applications. *Nat. Biotechnol.* **20**, 87-90. doi:10.1038/nbt0102-87
Neisch, A. L., Neufeld, T. P. and Hays, T. S. (2017). A STRIPAK complex mediates axonal transport of autophagosomes and dense core vesicles through PP2A regulation. *J. Cell Biol.* **216**, 1-21. doi:10.1083/jcb.201606082
Papagiannouli, F. and Mechler, B. M. (2009). *discs large* regulates somatic cyst cell survival and expansion in *Drosophila* testis. *Cell Res.* **19**, 1139-1149. doi:10.1038/cr.2009.71
Pardal, R., Clarke, M. F. and Morrison, S. J. (2003). Applying the principles of stem-cell biology to cancer. *Nat. Rev. Cancer* **3**, 895-902. doi:10.1038/nrc1232
Perezgasga, L., Jiang, J., Bolival, B., Hiller, M., Benson, E., Fuller, M. T. and White-Cooper, H. (2004). Regulation of transcription of meiotic cell cycle and terminal differentiation genes by the testis-specific Zn-finger protein *matotopetli*. *Development* **131**, 1691-1702. doi:10.1242/dev.01032
Pracheil, T. and Liu, Z. (2013). Tiered assembly of the yeast Far3-7-8-9-10-11 complex at the endoplasmic reticulum. *J. Biol. Chem.* **288**, 16986-16997. doi:10.1074/jbc.M113.451674
Pracheil, T., Thornton, J. and Liu, Z. (2012). TORC2 Signaling is antagonized by protein phosphatase 2a and the far complex in *Saccharomyces cerevisiae*. *Genetics* **190**, 1325-1339. doi:10.1534/genetics.111.138305
Reya, T., Morrison, S. J., Clarke, M. F. and Weissman, I. L. (2001). Stem cells, cancer, and cancer stem cells. *Nature* **414**, 105-111. doi:10.1038/35102167
Ribeiro, P. S., Josué, F., Wepf, A., Wehr, M. C., Rinner, O., Kelly, G., Tapon, N. and Gstaiger, M. (2010). Combined functional genomic and proteomic approaches identify a PP2A complex as a negative regulator of hippo signaling. *Mol. Cell* **39**, 521-534. doi:10.1016/j.molcel.2010.08.002
Richardson, H. E. and Portela, M. (2018). Modelling cooperative tumorigenesis in *Drosophila*. *BioMed Res. Int.* **2018**, 29. doi:10.1155/2018/4258387
Riesgo-Escovar, J. R. and Hafen, E. (1997). *Drosophila* Jun kinase regulates expression of *decapentaplegic* via the ETS-domain protein Aop and the AP-1

transcription factor DJun during dorsal closure. *Genes Dev.* **11**, 1717-1727. doi:10.1101/gad.11.13.1717

Ríos-Barrera, L. D. and Riesgo-Escovar, J. R. (2013). Regulating cell morphogenesis: the *Drosophila* Jun N-terminal kinase pathway. *Genesis* **51**, 147-162. doi:10.1002/dvg.22354

Robinson, B. S. and Moberg, K. H. (2011). *Drosophila* endocytic neoplastic tumor suppressor genes regulate Sav/Wts/Hpo signaling and the c-Jun N-terminal kinase pathway. *Cell Cycle* **10**, 4110-4118. doi:10.4161/cc.10.23.18243

Rohn, J. L., Sims, D., Liu, T., Fedorova, M., Schöck, F., Dopie, J., Vartiainen, M. K., Kiger, A. A., Perrimon, N. and Baum, B. (2011). Comparative RNAi screening identifies a conserved core metazoan actinome by phenotype. *J. Cell Biol.* **194**, 789-805. doi:10.1083/jcb.201103168

Rudrapatna, V. A., Bangi, E. and Cagan, R. L. (2013). A Jnk–Rho–Actin remodeling positive feedback network directs Src-driven invasion. *Oncogene* **33**, 2801-2806. doi:10.1038/onc.2013.232

Sakuma, C., Kawauchi, T., Haraguchi, S., Shikanai, M., Yamaguchi, Y., Gelfand, V. I., Luo, L., Miura, M. and Chihara, T. (2014). *Drosophila* Strip serves as a platform for early endosome organization during axon elongation. *Nat. Commun.* **5**, 5180-5180. doi:10.1038/ncomms6180

Sakuma, C., Okumura, M., Umehara, T., Miura, M. and Chihara, T. (2015). A STRIPAK component Strip regulates neuronal morphogenesis by affecting microtubule stability. *Sci. Rep.* **5**, 1-11. doi:10.1038/srep17769

Sakuma, C., Saito, Y., Umehara, T., Kamimura, K., Maeda, N., Mosca, T. J., Miura, M. and Chihara, T. (2016). The strip-hippo pathway regulates synaptic terminal formation by modulating actin organization at the *Drosophila* neuromuscular synapses. *Cell Rep.* **16**, 2289-2297. doi:10.1016/j.celrep.2016.07.066

Sarkar, A., Parikh, N., Hearn, S. A., Fuller, M. T., Tazuke, S. I. and Schulz, C. (2007). Antagonistic roles of Rac and Rho in organizing the germ cell microenvironment. *Curr. Biol.* **17**, 1253-1258. doi:10.1016/j.cub.2007.06.048

Schindelin, J., Arganda-Carreras, I., Frise, E., Kaynig, V., Longair, M., Pietzsch, T., Preibisch, S., Rueden, C., Saalfeld, S., Schmid, B. et al. (2012). Fiji: an open-source platform for biological-image analysis. *Nat. Methods* **9**, 676-682. doi:10.1038/nmeth.2019

Schulz, C., Wood, C. G., Jones, D. L., Tazuke, S. I. and Fuller, M. T. (2002). Signaling from germ cells mediated by the *rhomboid* homolog *stet* organizes encapsulation by somatic support cells. *Development* **129**, 4523-4534. doi:10.3410/f.1006866.121157

Schulz, C., Kiger, A. A., Tazuke, S. I., Yamashita, Y. M., Pantalena-Filho, L. C., Jones, D. L., Wood, C. G. and Fuller, M. T. (2004). A misexpression screen reveals rffects of *bag-of-marbles* and TGFβ class signaling on the *Drosophila* male germ-line stem cell lineage. *Genetics* **167**, 707-723. doi:10.1534/genetics.103.023184

Shi, Z., Jiao, S. and Zhou, Z. (2016). STRIPAK complexes in cell signaling and cancer. *Oncogene* **35**, 4549-4557. doi:10.1038/onc.2016.9

Shivdasani, A. A. and Ingham, P. W. (2003). Regulation of stem cell maintenance and transit amplifying cell proliferation by TGF-β signaling in *Drosophila* spermatogenesis. *Curr. Biol.* **13**, 2065-2072. doi:10.1016/j.cub.2003.10.063

Singh, S. R., Zhen, W., Zheng, Z., Wang, H., Oh, S.-W., Liu, W., Zbar, B., Schmidt, L. S. and Hou, S. X. (2006). The *Drosophila* homolog of the human tumor suppressor gene BHD interacts with the JAK-STAT and Dpp signaling pathways in regulating male germline stem cell maintenance. *Oncogene* **25**, 5933-5941. doi:10.1038/sj.onc.1209593

Smith, C. A., Farrah, T. and Goodwin, R. G. (1994). The TNF receptor superfamily of cellular and viral proteins: activation, costimulation, and death. *Cell* **76**, 959-962. doi:10.1016/0092-8674(94)90372-7

Takatsu, Y., Nakamura, M., Stapleton, M., Danos, M. C., Matsumoto, K., O'Connor, M. B., Shibuya, H. and Ueno, N. (2000). TAK1 participates in c-Jun N-terminal kinase signaling during *Drosophila* Development. *Mol. Cell. Biol.* **20**, 3015-3026. doi:10.1128/MCB.20.9.3015-3026.2000

Tang, Y., Geng, Q., Chen, D., Zhao, S., Liu, X. and Wang, Z. (2017). Germline proliferation is regulated by somatic endocytic genes via JNK and BMP signaling in *Drosophila*. *Genetics* **206**, 189-197. doi:10.1534/genetics.116.196535

Terry, N. A., Tulina, N., Matunis, E. and DiNardo, S. (2006). Novel regulators revealed by profiling *Drosophila* testis stem cells within their niche. *Dev. Biol.* **294**, 246-257. doi:10.1016/j.ydbio.2006.02.048

Tran, J., Brenner, T. J. and DiNardo, S. (2000). Somatic control over the germline stem cell lineage during *Drosophila* spermatogenesis. *Nature* **407**, 754-757. doi:10.1038/35037613

Uhlirova, M. and Bohmann, D. (2006). JNK- and Fos-regulated Mmp1 expression cooperates with Ras to induce invasive tumors in *Drosophila*. *EMBO J.* **25**, 5294-5304. doi:10.1038/sj.emboj.7601401

Vidal, M. (2010). The dark side of fly TNF. *Cell Cycle* **9**, 3851-3856. doi:10.4161/cc.9.19.13280

Voog, J., Sandall, S. L., Hime, G. R., Resende, L. P. F., Loza-Coll, M., Aslanian, A., Yates, J. R., III, Hunter, T., Fuller, M. T. and Jones, D. L. (2014). Escargot restricts niche cell to stem cell conversion in the *Drosophila* testis. *Cell Rep.* **7**, 722-734. doi:10.1016/j.celrep.2014.04.025

Wang, L., Li, Z. and Cai, Y. (2008). The JAK/STAT pathway positively regulates DPP signaling in the *Drosophila* germline stem cell niche. *J. Cell Biol.* **180**, 721-728. doi:10.1083/jcb.200711022

Wassarman, D. A., Solomon, N. M., Chang, H. C., Karim, F. D., Therrien, M. and Rubin, G. M. (1996). Protein phosphatase 2A positively and negatively regulates Ras1-mediated photoreceptor development in *Drosophila*. *Genes Dev.* **10**, 272-278. doi:10.1101/gad.10.3.272

White, A. C. and Lowry, W. E. (2014). Refining the role for adult stem cells as cancer cells of origin. *Trends Cell Biol.* **25**, 11-20. doi:10.1016/j.tcb.2014.08.008

Zeitlinger, J., Kockel, L., Peverali, F. A., Jackson, D. B., Mlodzik, M. and Bohmann, D. (1997). Defective dorsal closure and loss of epidermal *decapentaplegic* expression in *Drosophila fos* mutants. *EMBO J.* **16**, 7393-7401. doi:10.1093/emboj/16.24.7393

Zoller, R. and Schulz, C. (2012). The *Drosophila* cyst stem cell lineage. Partners behind the scenes? *Spermatogenesis* **2**, 1-13. doi:10.4161/spmg.21380

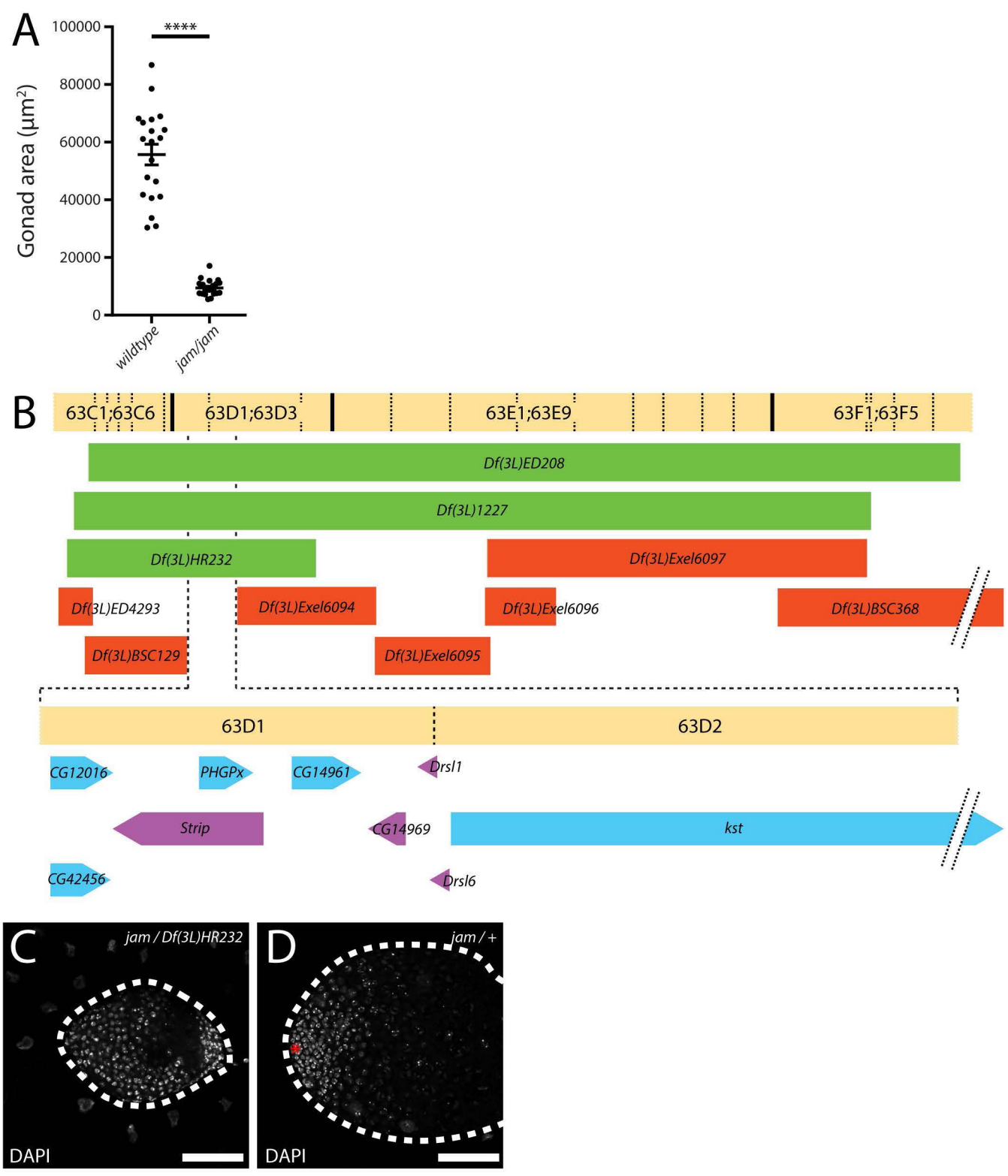

Figure S1. Deletion mapping to identify the lethal region containing *jam*. (A) Graph indicating the statistically significant reduction in area of *jam/jam* gonads compared to the *wildtype* ($p<0.0001$, represented by ****). Error bars = S.E.M. (B) Diagram representing cytological region 63C;63F of the *Drosophila* 3rd chromosome, and the coverage of deficiency stocks used to map the lethal region containing *jam*. Deficiency stocks that failed-to-complement *jam* are green, and those that complemented are red. (B,C) Gonads from transheterozygous *jam/Df(3L)HR232* (n=18/18) (C) and heterozygous *jam/+* (n=3/3) (D) animals, stained with DAPI. Where possible, an asterisk marks the hub. Dotted lines outline the gonads. Scale bars = 50µm.

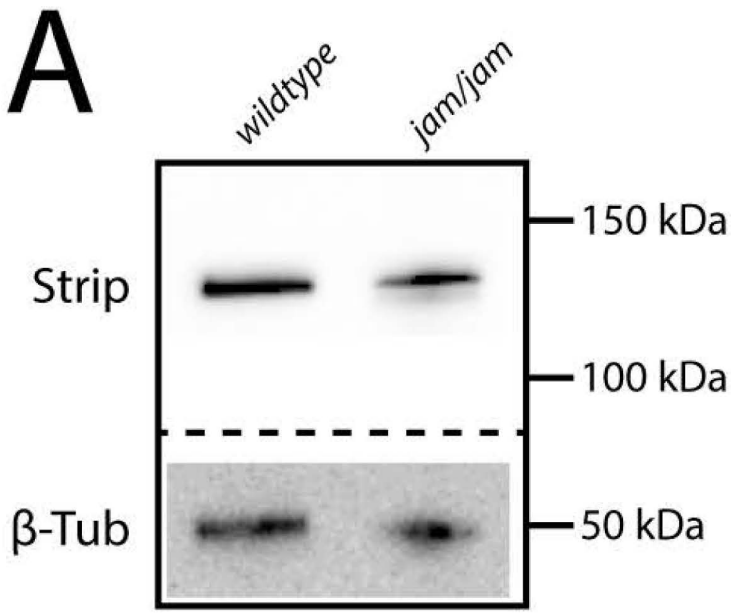

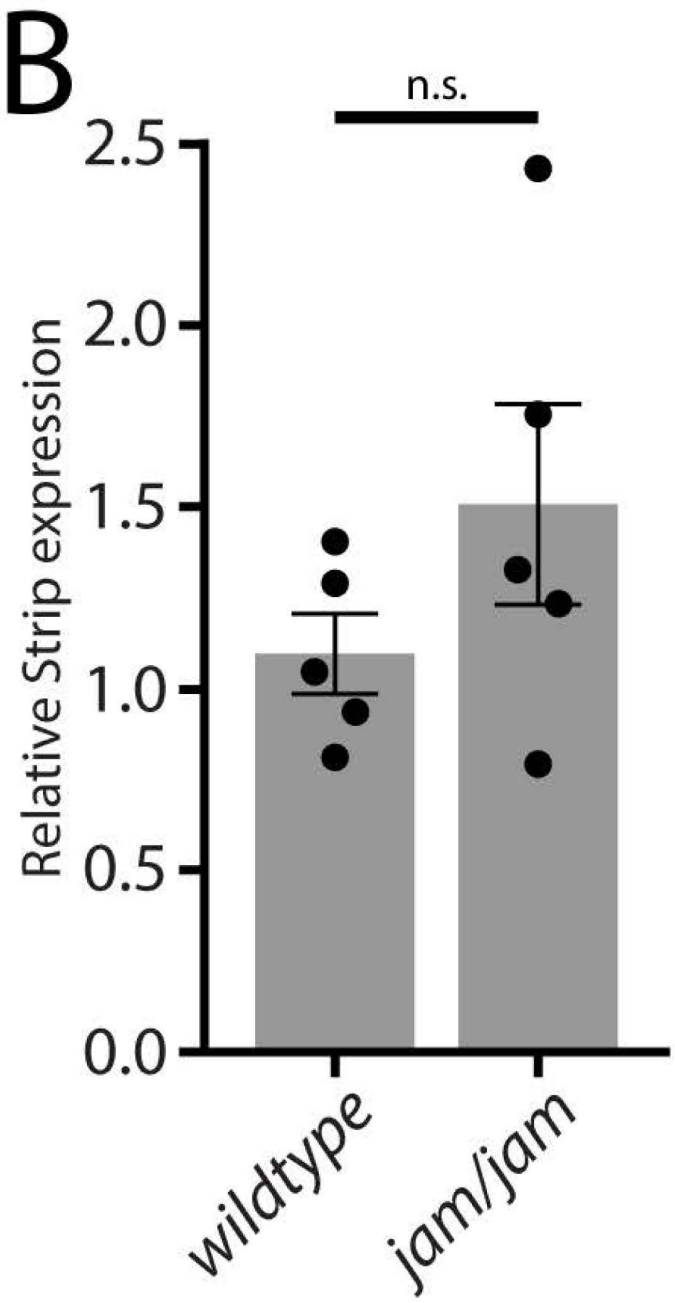

Figure S2. Strip^{jam} is translatable. (A) Western blotting for Strip revealed the protein in both *wildtype* and *jam/jam* tissues, at roughly 130 kDa (performed 5 times). β-Tubulin was used as a loading control. (B) Quantification of Strip expression relative to the loading control revealed no significant difference between the *wildtype* and the mutant (Student's t-test, $p>0.05$).

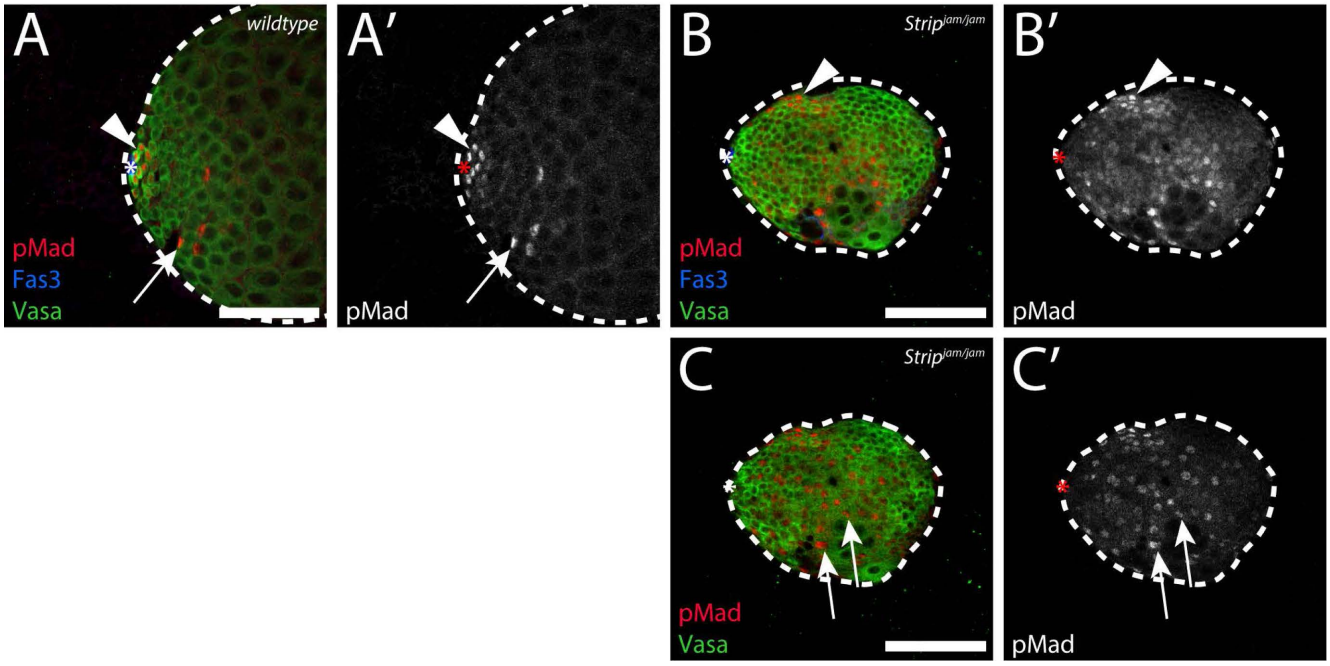

Figure S3. BMP signalling is disrupted in *Strip*$^{jam/jam}$ gonads. (A-B') *Wildtype* (n=21/21) (A,A') and *Strip*$^{jam/jam}$ (n=29/29) (B-C') gonads stained for pMad, Fas3, and Vasa. B and C are different Z-sections of the same gonad. Arrowheads and arrows indicate pMad-positive germline and somatic cells, respectively. Where possible, an asterisk marks the hub. Dotted lines outline the gonads. Scale bars = 50μm.

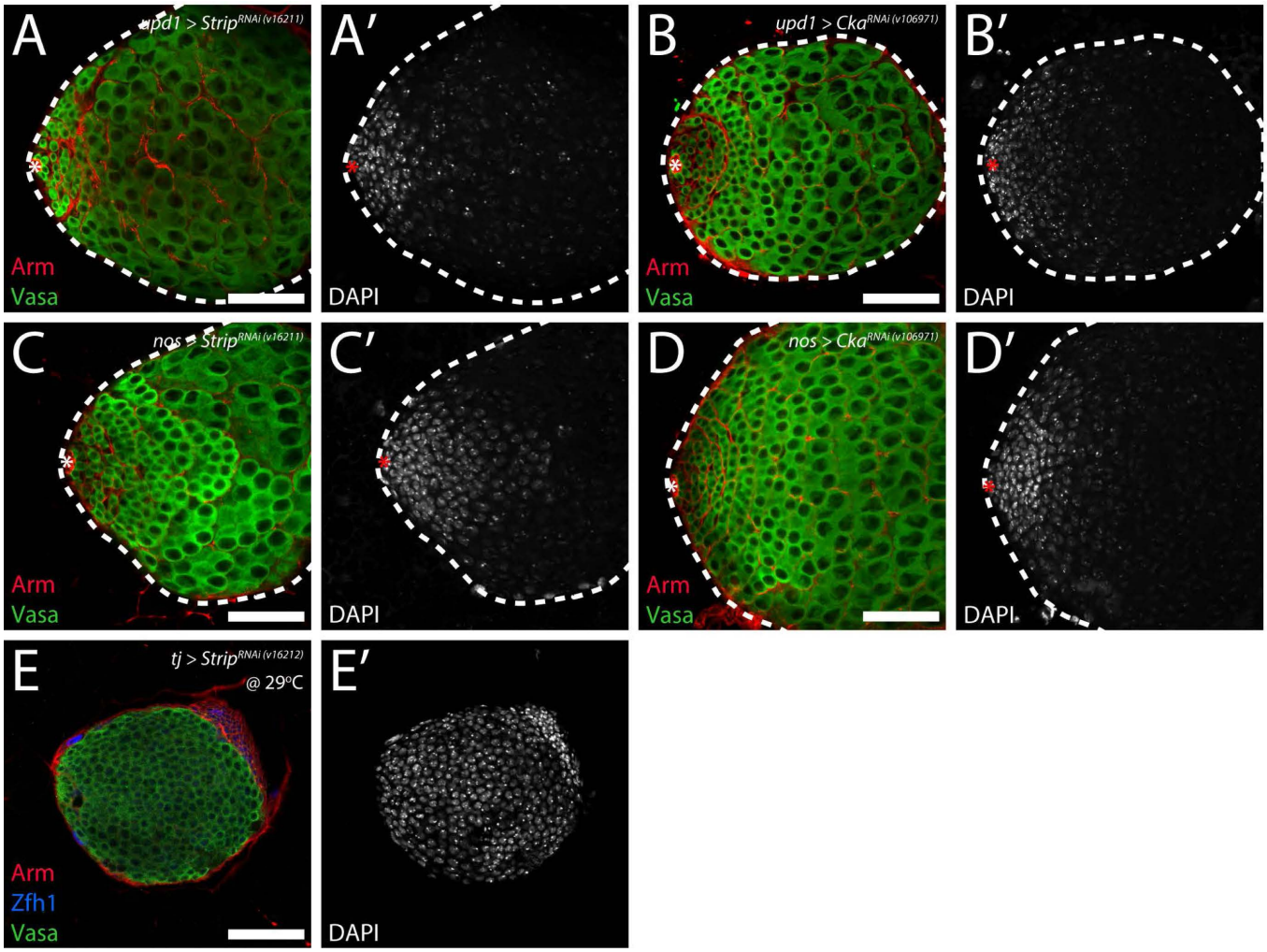

Figure S4. *Strip* and *Cka* are dispensable in the hub and germline cells. (A-D') Gonads from animals with hub or germline lineage expression of RNAi against *Strip* (v16211) or *Cka* (v106971), stained for Arm and Vasa, and with DAPI. (A-B') Hub cell specific expression of RNAi against *Strip* (n=28/28) (A,A') and *Cka* (n=7/7) (B,B') driven using *upd1-GAL4*. (C-D') Early germline cell specific expression of RNAi against *Strip* (n=14/14) (C,C') and *Cka* (n=14/14) (D,D') driven using *nos-GAL4*. (E,E') Gonads with somatic lineage expression of RNAi against *Strip* (v16212) via *tj-GAL4* , stained for Arm, Zfh1, and Vasa, and with DAPI. The phenotype induced via homozygosity for $Strip^{jam}$ or knockdown of *Strip* using *C587-GAL4* is replicated using *tj-GAL4*. Note that the *nos-GAL4* driver stock also includes a *UAS-GAL4* construct to strengthen expression. Where possible, an asterisk marks the hub. Dotted lines outline the gonads. Scale bars = 50μm.

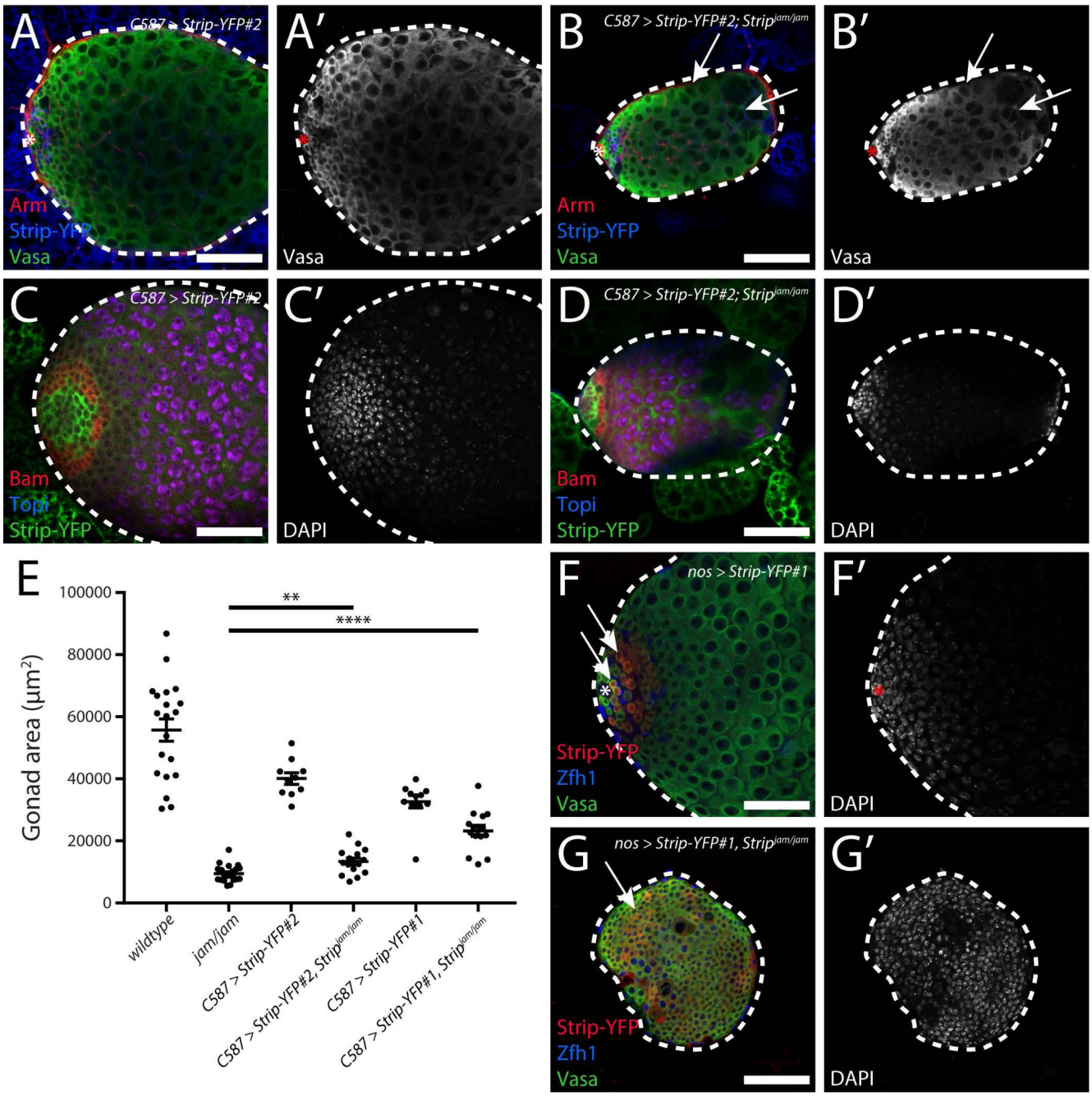

Figure S5. Somatic cell expression of *Strip-YFP* partially rescues *Strip$^{jam/jam}$*. (A-D') Gonads from animals with somatic lineage expression of *Strip-YFP#2* in both *wildtype* (n=23/23) (A,A',C,C') and *Strip$^{jam/jam}$* (n=42/42) (B,B',D,D') backgrounds, stained for Arm and Vasa, or for Bam and Topi with DAPI. Arrows indicate individualised, yet differentiated, germline cells. Note the apparent magenta staining in C and D is due to stronger than usual background staining in the Bam (red) channel. (E) Graph indicating the statistically significant increase in the area of *Strip$^{jam/jam}$* gonads after somatic lineage expression of *Strip-YFP#1* ($p<0.0001$, represented by ****) and *Strip-YFP#2* ($p<0.01$, represented by **). (F-G') Gonads from animals expressing *Strip-YFP#1* in the somatic lineage in both *wildtype* (n=9/9) (E,E') and *Strip$^{jam/jam}$* (n=16/16) (F,F') backgrounds, stained for Zfh1 and Vasa. Arrows indicate Strip-YFP expression in the germline cells. Where possible, an asterisk marks the hub. Dotted lines outline the gonads. Scale bars = 50µm.

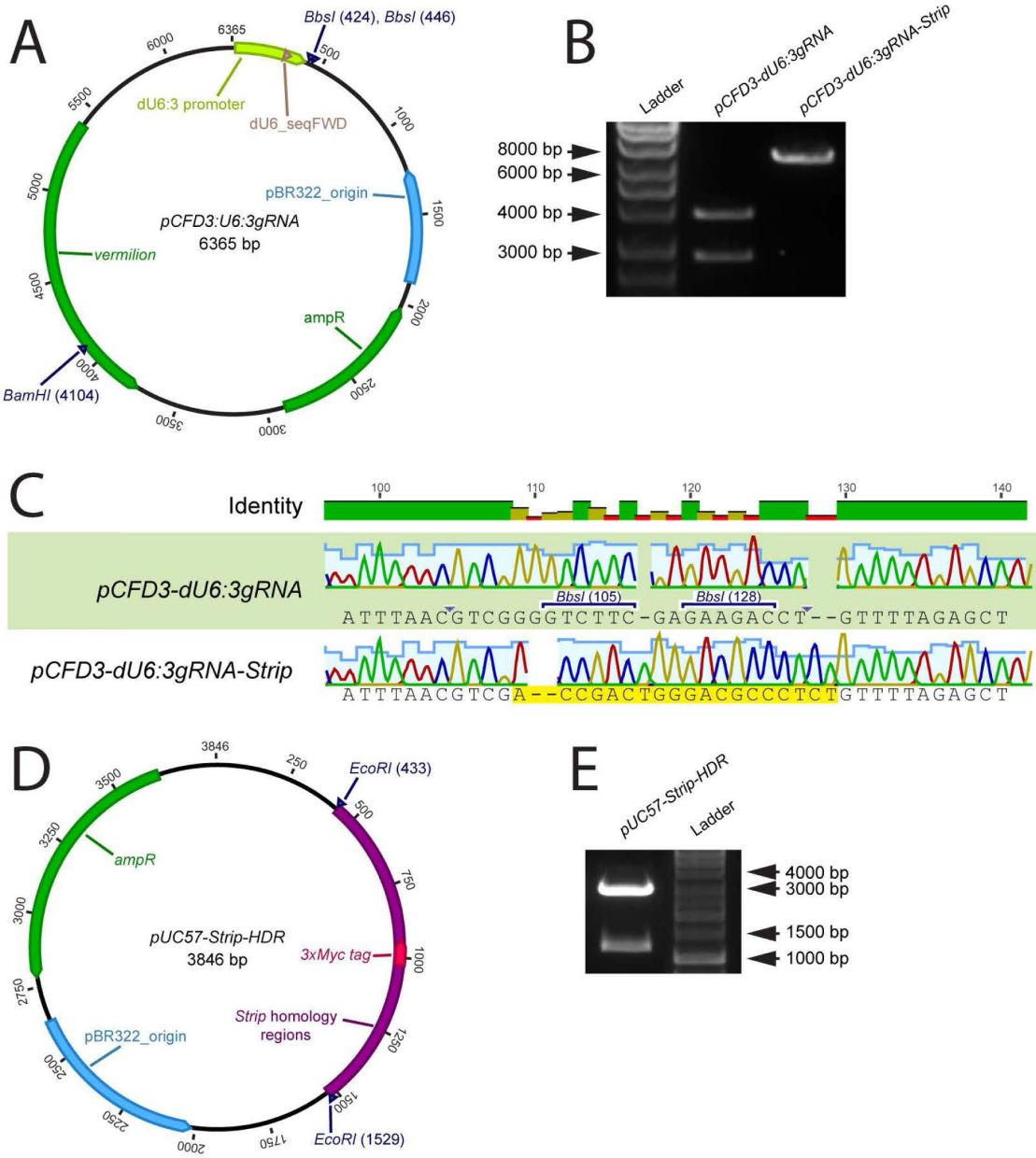

Figure S6. CRISPR/Cas9 epitope tagging of Strip. (A-C) *pCFD3:U6:3-gRNA* was modified to contain the gRNA sequence for targeting *Strip*. (A) Plasmid map of unmodified *pCFD3:U6:3-gRNA*. The desired gRNA sequence was inserted into the *BbsI* sites. "dU6:3 promoter" is the gRNA promoter sequence, and "dU6_seqFWD" denotes the position of the forward primer used for sequencing. (B) Gel electrophoresis of unmodified and modified *pCFD3:U6:3-gRNA* digested with *BamHI* and *BbsI* restriction endonucleases. Loss of BbsI sites indicates successful insertion of the gRNA sequence. (C) Sequence data for unmodified *pCFD3:U6:3-gRNA* and modified *pCFD3:U6:3-gRNA-Strip*. The *pCFD3:U6:3-gRNA-Strip* sequence was aligned to the *pCFD3:U6:3-gRNA* reference sequence. The modified sequence reflects the gel electrophoresis result, showing successful insertion of the gRNA sequence (highlighted in yellow), and loss of the *BbsI* cut sites. (D,E) A repair template consisting of a homology region for *Strip* and a *3×Myc tag* at the appropriate site was synthesised in a *pUC57-simple* (*pUC57*) backbone. (D) Plasmid map of *pUC57-Strip-HDR*. (E) Gel electrophoresis of *pUC57-Strip-HDR* digested with *EcoRI* to release the 1090bp repair template. In each plasmid map "pBR322_origin" refers to the plasmid origin of replication sequence and "*ampR*" refers to the ampicillin resistance gene. Plasmid maps were generated in Geneious v.8 (Kearse et al., 2012). (F-G'') *Strip-Myc*$^{2\text{-}38\text{-}4\text{-}1}$ gonads (n=9/9) stained for the Myc epitope tag, Zfh1, and Vasa, at both regular (F-F'') and higher (G-G'') magnifications. Arrows indicate patches of strong Strip-Myc expression. Where possible, an asterisk marks the hub. Dotted lines outline the gonads. Scale bars = 50μm.

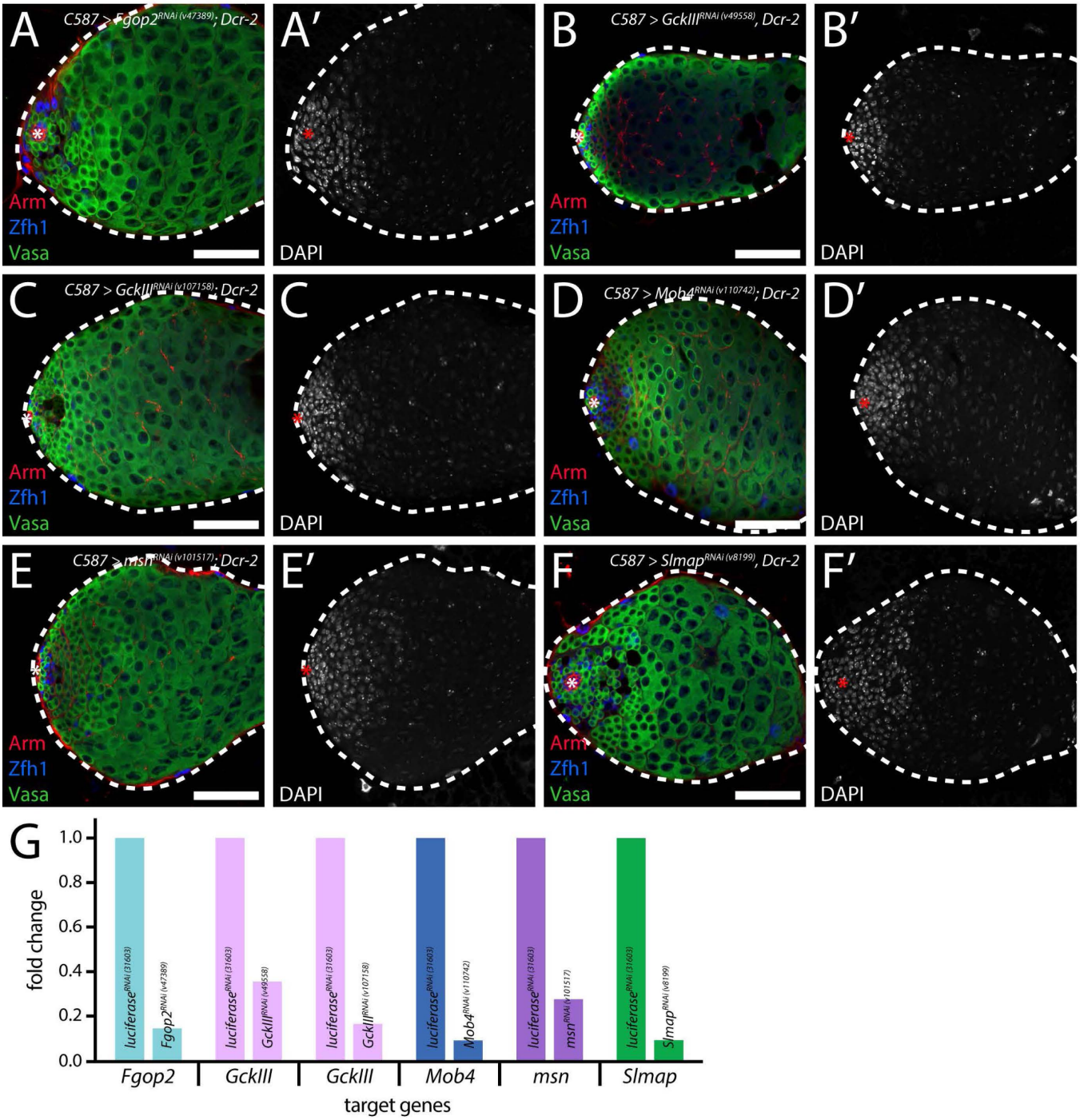

Figure S7. Somatic cell knockdown of other STRIPAK components does not affect spermatogenesis. (A-H') Gonads from animals with somatic lineage expression of RNAi against STRIPAK complex components, alongside *Dcr-2*, in an otherwise *wildtype* background, stained for Arm, Zfh1, and Vasa, and with DAPI. (A,A') RNAi (v47389) against *Fgop2* (n=4/4). (B,B') RNAi (v49558) against *GckIII* (n=16/16). (C,C') RNAi (v107158) against *GckIII* (n=6/6). (D,D') RNAi (v110742) against *Mob4* (n=45/46). (E,E') RNAi (v101517) against *msn* (n=12/12). (F,F') RNAi (v8199) against *Slmap* (n=42/45). (G) Efficacy of STRIPAK RNAi lines measured via RT-qPCR. Pictured is the amount of target mRNA after knockdown of the STRIPAK component genes, relative to that from a *luciferase* knockdown control (n>10 animals per genotype). Where possible, an asterisk marks the hub. Dotted lines outline the gonads. Scale bars = 50μm.

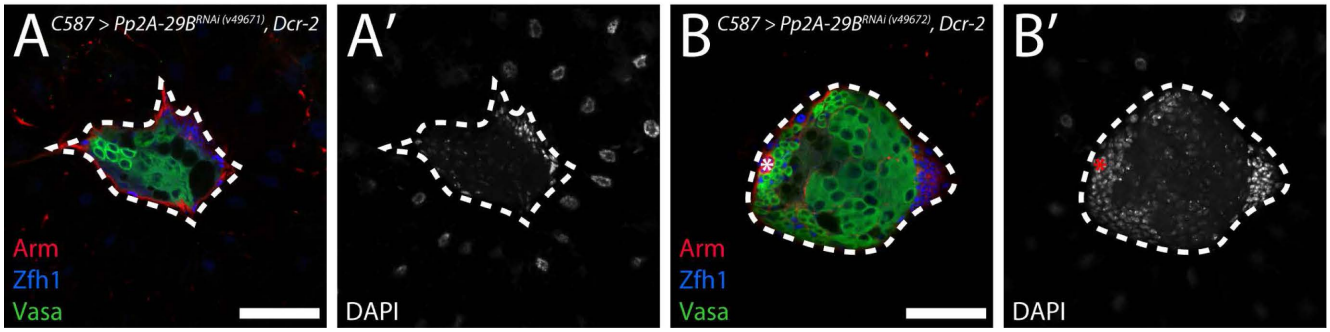

Figure S8. Somatic cell knockdown of *Pp2A-29B* leads to early germline cell loss. (A-B') Gonads from animals with somatic lineage expression of *Dcr-2*, alongside RNAi against *Pp2A-29B* v49671 (n=9/9) (A,A') and v49672 (n=9/9) (B,B'), stained for Arm, Zfh1, and Vasa, and with DAPI. Where possible, an asterisk marks the hub. Dotted lines outline the gonads. Scale bars = 50μm.

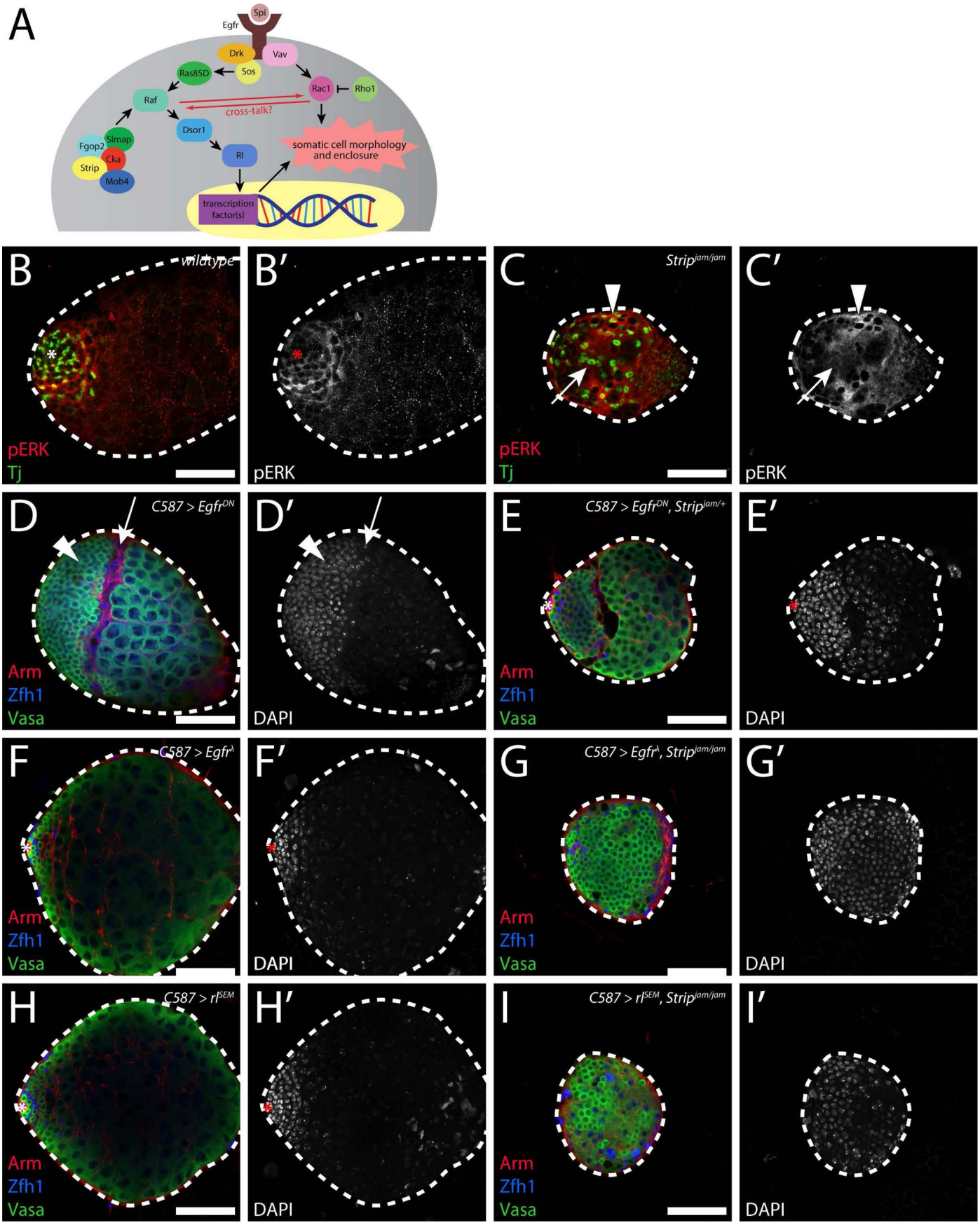

Figure S9. *Strip* does not genetically interact with the EGFR signalling pathway in the gonad. (A) Diagram of the bifurcated EGFR signalling pathway regulating *Drosophila* spermatogenesis. STRIPAK complex members have been shown to act as positive regulators of the pathway in *Drosophila* S2 cells, as well as adult wing and eye tissues. (B-C') *Wildtype* (n=26/26) (B,B') and $Strip^{jam/jam}$ (n=29/29) (C,C') gonads stained for pERK and Tj. Arrow indicates a pERK-positive somatic cell; arrowhead indicates a pERK-negative somatic cell. No obvious change in pERK levels was observed, although somatic cells in the mutant sporadically did not express pERK. (D-I') Gonads from animals with somatic lineage expression of various transgenes, stained for Arm, Zfh1, and Vasa, and with DAPI. (D-E') Gonads from animals expressing $Egfr^{DN}$ in the somatic lineage in both *wildtype* (n=17/21) (D,D') and $Strip^{jam/+}$ (n=19/22) (E,E') backgrounds. Arrows indicate non-enclosing somatic cells; arrowheads indicate supernumerary early germline cells. Being additionally heterozygous for $Strip^{jam}$ did not enhance the $Egfr^{DN}$-induced phenotype. (F-G') Gonads from animals expressing $Egfr^{\lambda}$ in the somatic lineage in both *wildtype* (n=7/7) (F,F') and $Strip^{jam/jam}$ (n=13/13) (G,G') backgrounds. $Egfr^{\lambda}$ expression did not alter the mutant phenotype. (H-I') Gonads from animals expressing rl^{SEM} in the somatic lineage in both *wildtype* (n=12/12) (H,H') and $Strip^{jam/jam}$ (n=6/6) (I,I') backgrounds. rl^{SEM} expression did not alter the mutant phenotype. Where possible, an asterisk marks the hub. Dotted lines outline the gonads. Scale bars = 50μm.

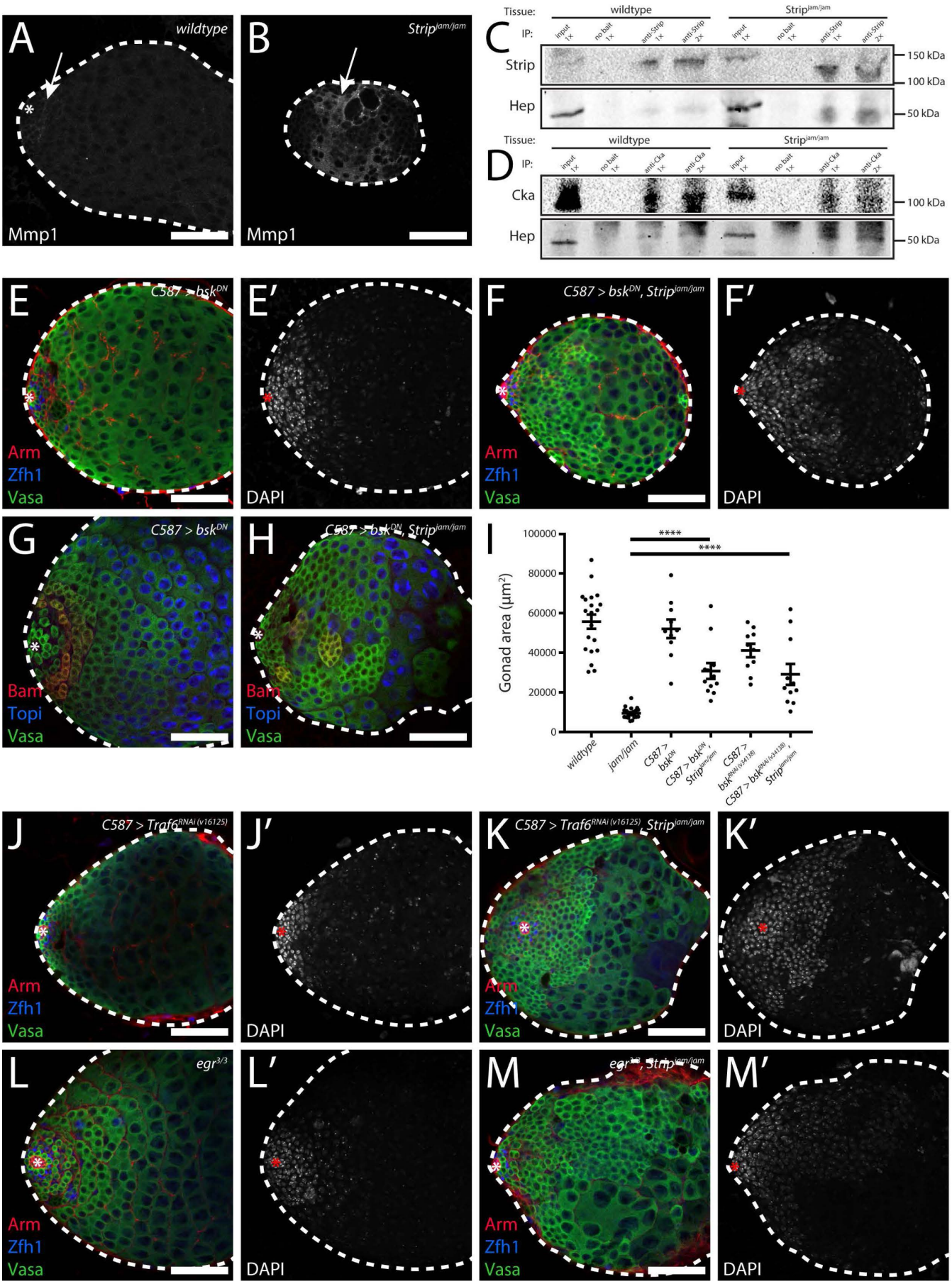

Figure S10. Hep physically interacts with both Strip and Cka in both *wildtype* and *Strip$^{jam/jam}$* gonads.

(A,B) *Wildtype* (n=10/10) (A) and *Strip$^{jam/jam}$* (n=12/12) (B) gonads stained for Mmp1. Arrows indicate Mmp1 expression. (C,D) In both *wildtype* and *Strip$^{jam/jam}$* tissue extracts, Hep immunoprecipitated when baited with either anti-Strip (C) or anti-Cka (D) (each performed 2 times – further assays were limited by our having only small quantities of these non-commercial antibodies, which also partly explains our inability to obtain "cleaner" blots, alongside stripping and re-probing of each blot contributing to a degradation of signal quality). (E-H', J-M') Gonads from animals with somatic lineage expression of various transgenes, stained variously for Arm, Zfh1, Bam, Topi, and Vasa, and with DAPI. (E-F') Expressing *bsk^{DN}* in both *wildtype* (n=20/20) (E,E',G) and *Strip$^{jam/jam}$* (n=34/35) (F,F',H) backgrounds rescues somatic and germline morphologies, as well as germline differentiation marker expression. (I) Graph indicating the statistically significant increase in the area of *Strip$^{jam/jam}$* gonads after somatic lineage expression of either RNAi against *bsk* and *bskDN* (both $p<0.0001$, represented by ****). (J-K') Expressing RNAi against *Traf6* in both *wildtype* (n=10/10) (J,J') and *Strip$^{jam/jam}$* (n=16/16) (K,K') backgrounds. (L-M') Gonads from animals homozygous for *egr^{3}* in *wildtype* (n=7/7) (L,L') and *Strip$^{jam/jam}$* (n=21/21) (M,M') backgrounds, stained for Arm, Zfh1, and Vasa, and with DAPI. Where possible, an asterisk marks the hub. Dotted lines outline the gonads. Scale bars = 50μm.

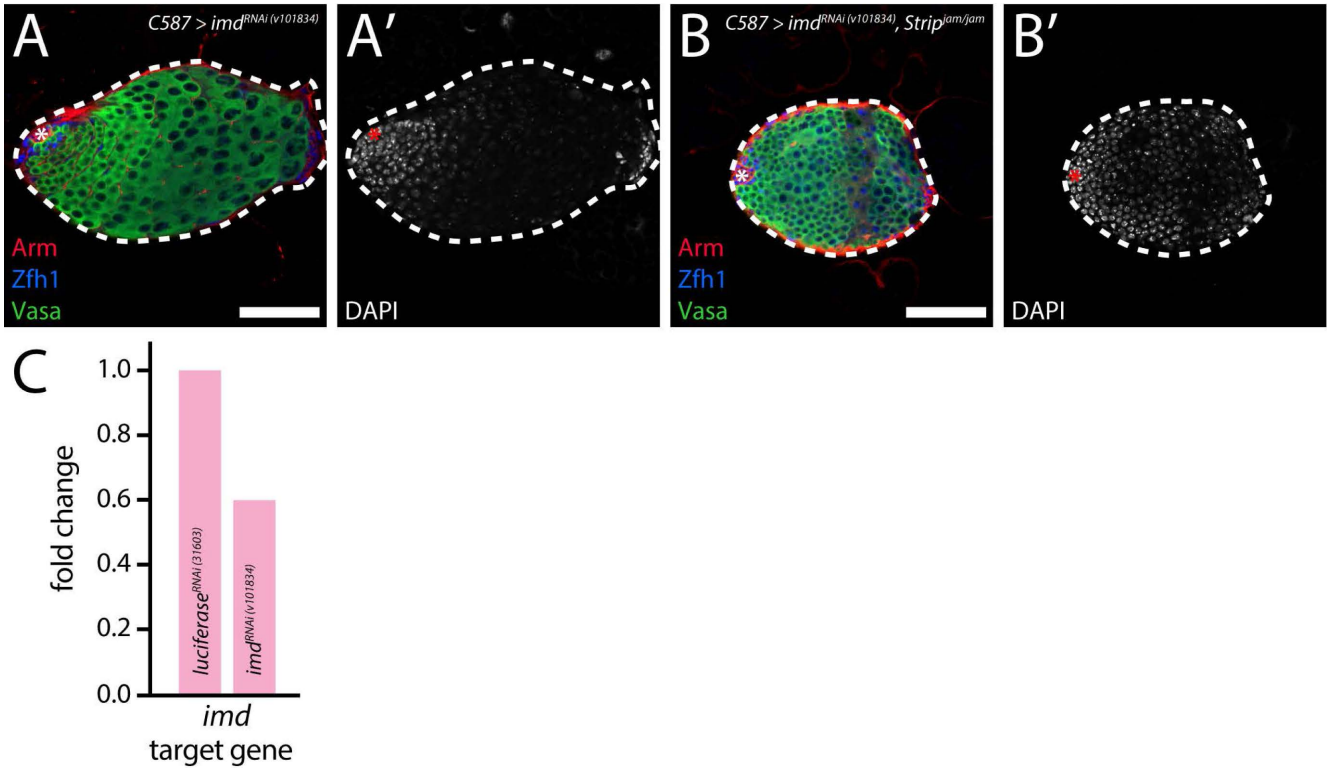

Figure S11. IMD signalling is dispensable during JNK signalling in *Strip*$^{jam/jam}$ gonads. (A-B') Gonads from animals with somatic lineage expression of RNAi against *imd* in both *wildtype* (n=7/7) (G,G') and *Strip*$^{jam/jam}$ (n=16/16) (H,H') backgrounds, stained for Arm, Zfh1, and Vasa, and with DAPI. (C) Efficacy of RNAi against *imd* measured via RT-qPCR. Pictured is the amount of *imd* mRNA after *imd* knockdown relative to that in a *luciferase* knockdown control (n>10 animals per genotype). Where possible, an asterisk marks the hub. Dotted lines outline the gonads. Scale bars = 50μm.

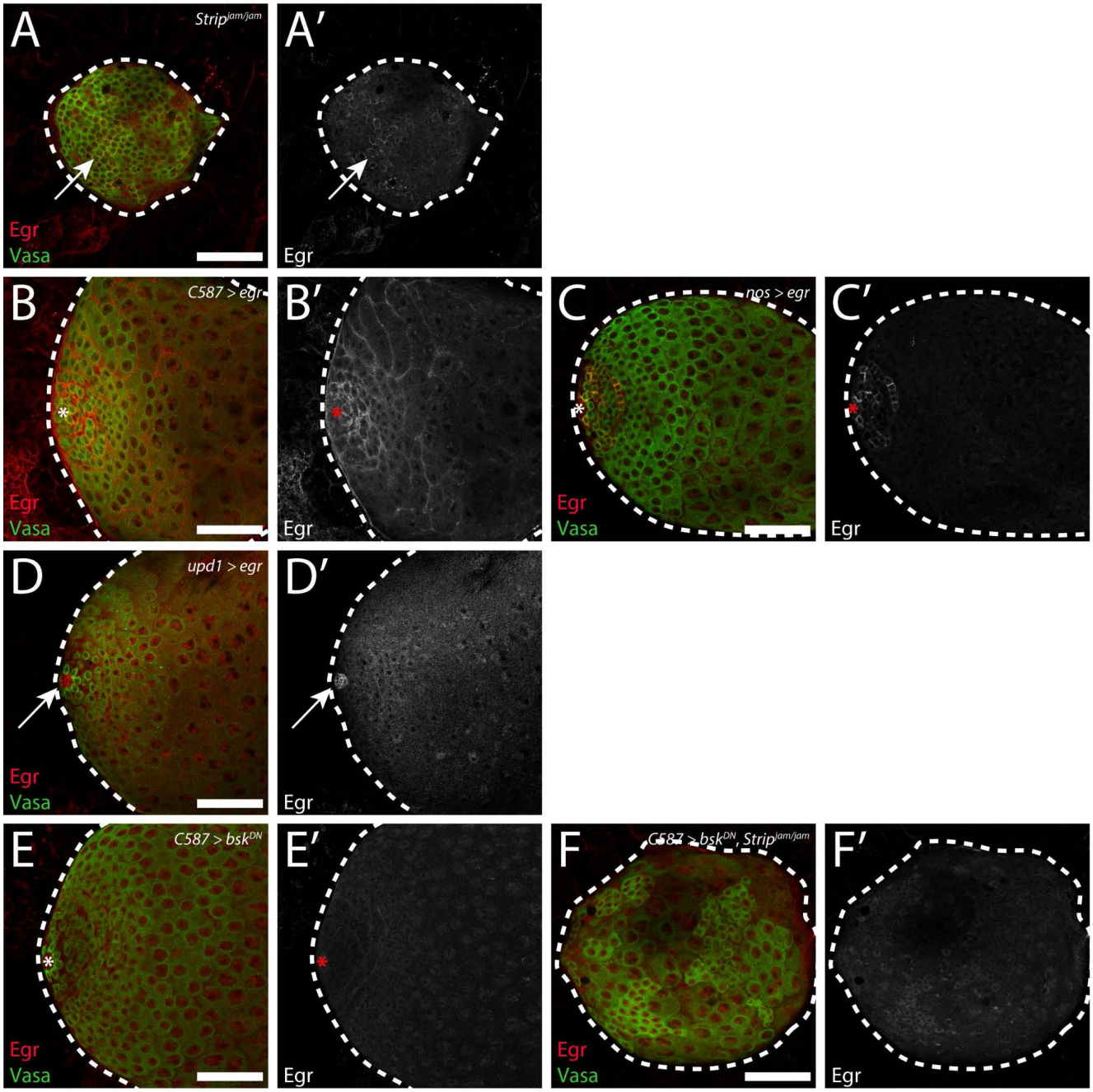

Figure S12. Egr expression is elevated in *Strip*$^{jam/jam}$ gonads. (A,A') *Strip*$^{jam/jam}$ gonads stained for Egr and Vasa. Arrows indicate concentrations of Egr expression in the cytoplasm of some germline cells. (B-F') Gonads from animals expressing various transgenes, stained for Egr and Vasa. (B-D') Expressing *egr* in the somatic (n=5/5) (B,B'), germline (n=11/11) (C,C'), and hub (n=12/12) (D,D') lineages in a *wildtype* background. Inducing *egr* expression does not alter the gonad phenotype. (E-F') Expressing *bsk*^{DN} in the somatic lineage in both *wildtype* (n=10/10) (E,E') and *Strip*$^{jam/jam}$ (n=13/13) (F,F') backgrounds. Where possible, an asterisk marks the hub, except for D,D', where an arrow marks the hub. Dotted lines outline the gonads. Scale bars = 50μm.s

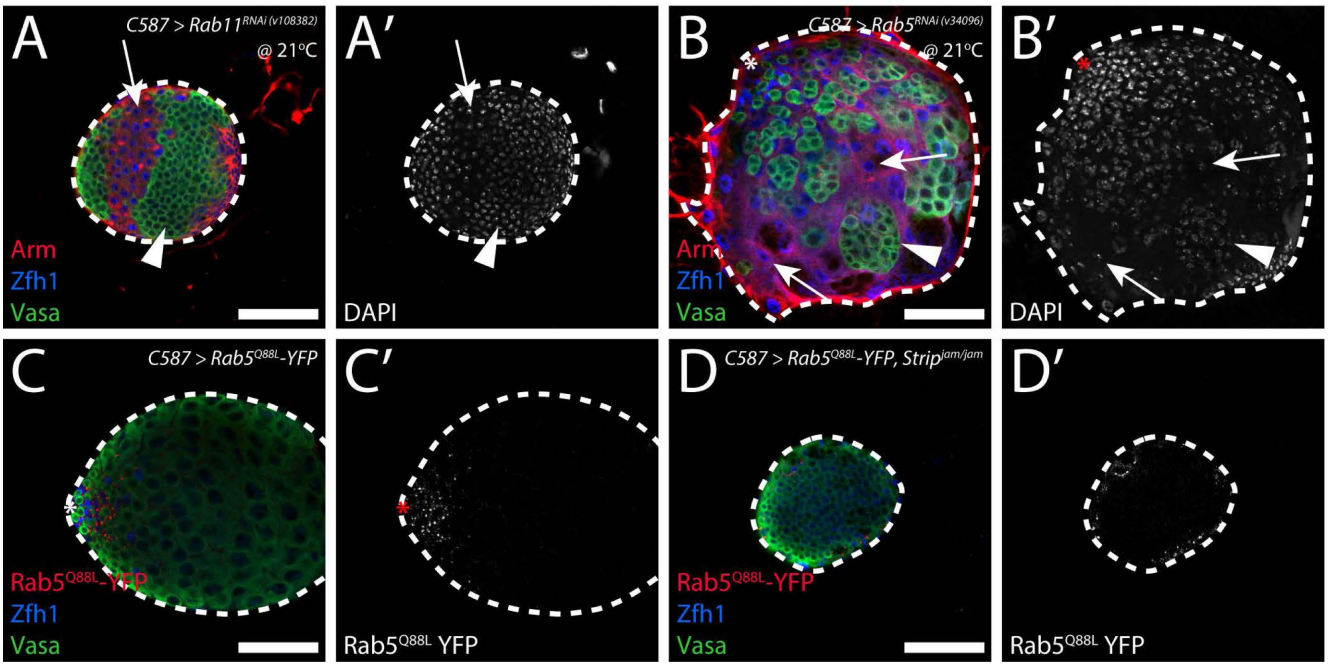

Figure S13. Endocytosis components are necessary during spermatogenesis, but do not interact genetically with Strip. (A-B') Gonads from animals with somatic lineage expression of various transgenes, stained for Arm, Zfh1, and Vasa, and with DAPI. Expressing RNAi against *Rab11* (n=13/13) results in dissociated somatic cells and ectopic early germline cells (A,A'). Arrows indicate non-enclosing somatic cells; arrowheads indicate supernumerary early germline cells. Expressing RNAi against *Rab5* (n=16/16) results in overproliferating cysts and some dissociated somatic cells (B,B'). Arrows indicate non-enclosing somatic cells; arrowheads indicate an overproliferating cyst. Note the apparent magenta staining is due to stronger than usual background staining in the Zfh1 (blue) channel. (C-D') Gonads from animals with somatic lineage expression of YFP tagged $Rab5^{Q88L}$, in both *wildtype* (n=35/35) (C,C') and $Strip^{jam/jam}$ (n=16/16) (D,D') backgrounds, stained for Zfh1 and Vasa. Where possible, an asterisk marks the hub. Dotted lines outline the gonads. Scale bars = 50μm.

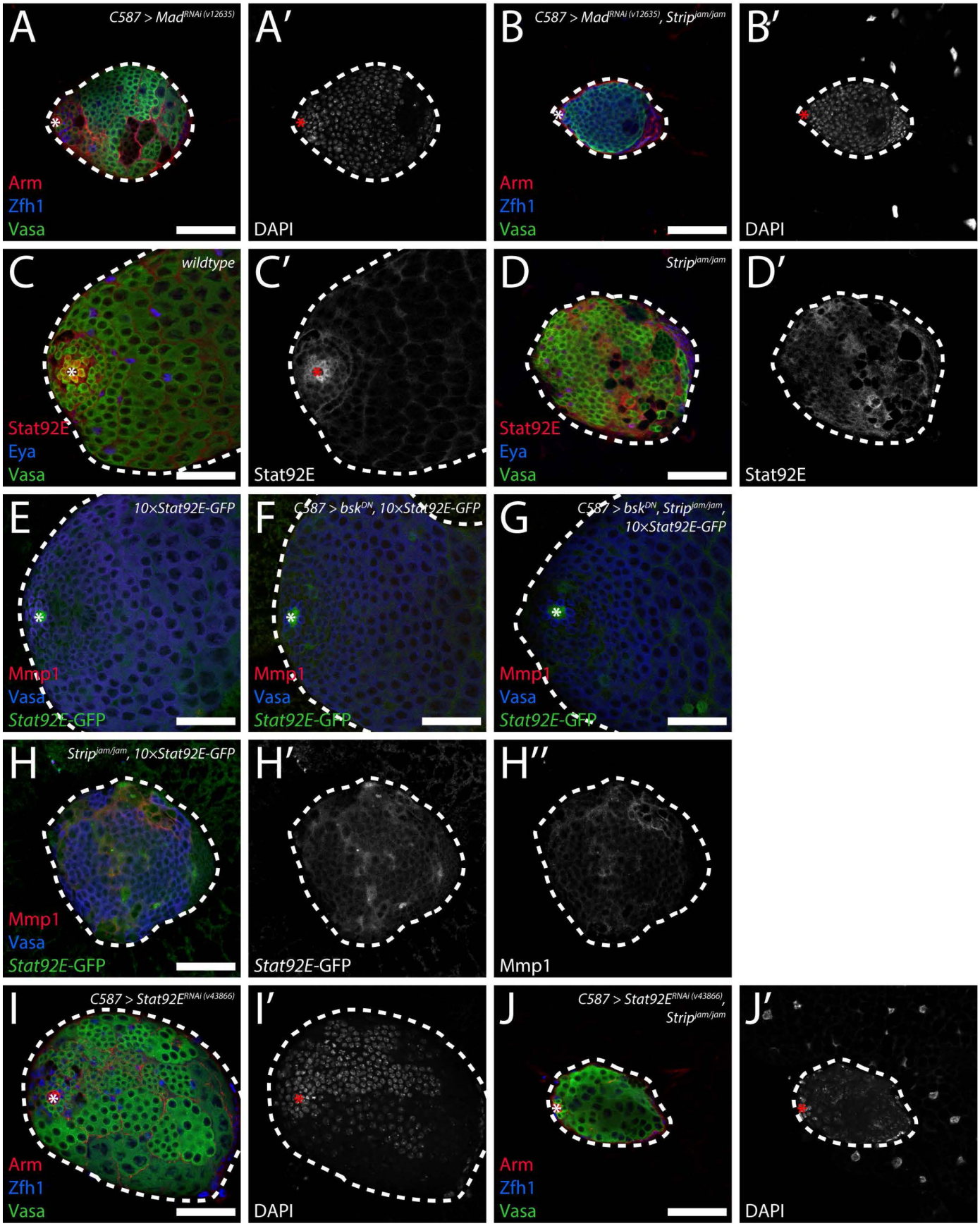

Figure S14. Jak-STAT and TGF-β signalling components do not genetically interact with *Strip*. (A-B'') Gonads from animals with somatic lineage expression of RNAi against *Mad*, stained for Arm, Zfh1, and Vasa, and with DAPI. In a *wildtype* background (n=9/9) (A,A''), *Mad* knockdown led to ectopic spermatogonia TA divisions, and in a $Strip^{jam/jam}$ background (n=10/10) (B,B'') it did not rescue the mutant phenotype. (C-D'') *Wildtype* (n=9/9) (C,C'') and $Strip^{jam/jam}$ (n=11/11) (D,D'') gonads stained for Stat92E, Eya, and Vasa. Stat92E expression appeared greater in the somatic cells of $Strip^{jam/jam}$ gonads. (E-H'') Gonads from animals heterozygous for *10×Stat92E-GFP*, stained for Mmp1 and Vasa. With no additional transgene expression (n=5/5) (E) or with somatic cell expression of bsk^{DN} (n=6/6) (F) in a *wildtype* background, or with somatic cell expression of bsk^{DN} in a $Strip^{jam/jam}$ background (n=6/6) (G), GFP expression appears to be limited to the hub, while in a $Strip^{jam/jam}$ background with no additional transgene expression (n=7/7) (H-H'') GFP is strongly expressed in the somatic cells and co-localises with Mmp1. (I-J'') Gonads from animals with somatic lineage expression of RNAi against *Stat92E*, stained for Arm, Zfh1, and Vasa, and with DAPI. In both *wildtype* (n=6/9) (I,I'') and $Strip^{jam/jam}$ (n=14/24) (J,J'') backgrounds, *Stat92E* knockdown led to early germline cell loss, and it did not rescue the mutant phenotype. Where possible, an asterisk marks the hub. Dotted lines outline the gonads. Scale bars = 50μm.